



## รายงานวิจัยฉบับสมบูรณ์

### โครงการ

การวิเคราะห์การสั่นสะเทือนของระบบไมโครแบร์ริ่งสปินเดิลที่มีแรงพลศาสตร์ในแบร์ริ่งเป็นแรงกระจาย

โดย รองศาสตราจารย์ ดร. ฐิติมา จินตนาวัน และคณะ

### รายงานวิจัยฉบับสมบูรณ์

โครงการ การวิเคราะห์การสั่นสะเทือนของระบบไมโครแบร์ริ่งสปินเดิลที่มีแรงพลศาสตร์ในแบร์ริ่งเป็นแรงกระจาย

คณะผู้วิจัย

สังกัด

1 รองศาสตราจารย์ ดร. จูิติมา จินตนาวัน

2 ศาสตราจารย์ ดร. วริทธิ์ อึ๊งภากรณ์

จุฬาลงกรณ์มหาวิทยาลัย

จุฬาลงกรณ์มหาวิทยาลัย

สนับสนุนโดยสำนักงานคณะกรรมการอุดมศึกษา และสำนักงานกองทุนสนับสนุนการวิจัย (ความเห็นในรายงานนี้เป็นของผู้วิจัย สกอ. และ สกว. ไม่จำเป็นต้องเห็นด้วยเสมอไป)

#### **Abstract**

This research proposes a new model of dynamic bearing forces for a bearing spindle system where the aspect ratio of the bearing width to the shaft length is significant, and the shaft is flexible. In this case the journal bearing functions as a continuous support, providing *distributed* restoring and damping forces. The applications can be found in the micro bearing-spindle systems such as hard disk drives (HDD) spindles. To characterize the distributed dynamic forces of the journals, the distribution functions of the stiffness and damping coefficients were determined along the bearing length through the perturbation of Reynold's equations. The dynamic model of the distributed bearing forces was then implemented in HDD spindle system. The mathematical model of the whole disk-spindle systems in HDD is developed for accurately predicting the transverse vibration. Vibration analysis reveals that the spindle model with distributed bearing forces predicts the same natural frequencies for all transverse modes but higher modal damping of the rocking modes, when compared to the values predicted by the conventional model with discrete bearing forces. The difference in damping prediction is clearer for the flexible-shaft spindle whose ratio of the bearing width to the shaft length becomes larger.

#### บทคัดย่อ

โครงการ การวิเคราะห์การสั่นสะเทือนของระบบไมโครแบร์ริ่งสปินเดิล ที่มีแรงพลศาสตร์ในแบร์ริ่งเป็นแรงกระจายนี้ มี วัตถุประสงค์ เพื่อพัฒนาแบบจำลองทางพลศาสตร์ของระบบดิสค์สปินเดิลขนาดเล็ก โดยพิจารณาแรงในแบร์ริ่งเป็นชนิด แรงกระจาย ซึ่งแบบจำลองดังกล่าวจะสามารถนำไปใช้ในการทำนายการสั่นสะเทือนของสปินเดิลไดร์วขนาดเล็กได้ เหมาะสม เนื่องจากลักษณะแบร์ริ่งในระบบสปินเดิลขนาดเล็ก จะมีค่าอัตราส่วนของความกว้างต่อความยาวเพลาสูง ทำ ให้ไม่สามารถพิจารณาแรงที่เกิดจากแบร์ริ่งเป็นแรงกระทำแบบจุด จากแนวคิดดังกล่าว งานวิจัยนี้ได้พัฒนาแบบจำลอง ทางพลศาสตร์ของแรงกระจายในแบร์ริ่ง ชนิด herringbone grooved journal bearings (HGJB) และพิจารณาหาฟังก์ชั่น การกระจายของค่าสัมปสิทธิ์ทางพลศาสตร์ของแบร์ริ่ง ซึ่งแสดงคุณลักษณะของแรงกระจายนี้ตามความสัมพันธ์ของ สมการ Reynold และขั้นตอนต่อมา ได้นำผลฟังก์ชั่นการกระจายของค่าสัมปสิทธิ์ของแบร์ริ่งนี้ ไปใช้เพื่อพัฒนา แบบจำลองทางพลศาสตร์ของระบบดิสค์สปินเดิล โดยใช้หลักการ Lagrange's Dynamics แบบจำลองที่พัฒนาขึ้นใหม่นี้ จะใช้ในการทำนายการสั่นสะเทือนของสปินเดิลไดร์วในฮาร์ดดิสค์ ซึ่งเป็นระบบสปินเดิลขนาดเล็ก ได้แม่นยำขึ้น เมื่อ เทียบกับผลการทำนายโดยแบบจำลองที่มีอยู่เดิม ที่พิจารณาแรงในแบร์ริ่งเป็นชนิดแรงกระทำแบบจุด และจะเป็น ประโยชน์ในการออกแบบขนาด และตำแหน่งของแบร์ริ่ง เพื่อลดการสั่นสะเทือนได้แม่นยำขึ้น

### **Contents**

Abstract	2
Contents	3
Chapter 1: Executive summary	4
1) Motivation and problem statement	4
2) Objectives	5
3) Research methodology	5
4) Outcome of this research	6
Chapter 2: Detail of Research Work	7
1) Introduction	7
2) Dynamic model of distributed forces in herringbone groove journal bearings (HGJB)	9
3) Mathematical model of hard disk drive spindle system with distributed bearing forces	18
4) Vibration analysis	19
5) Conclusions	24
6) References	25
Appendix	26

#### Chapter 1

#### **Executive Summary**

#### 1) Motivation and problem statement

Micro bearing-spindle systems are found in many applications such as hard disk drives (HDD), precision instruments, high-speed CNC machines, and dental instrument. For various micro spindles such as hard disk spindles, herringbone grooved journal bearings (HGJBs) are currently used to provide restoring and damping forces in the radial direction. Grooves in journal bearings are designed to improve half-speed whirl stability. The dynamic forces in the journal bearings, including HGJBs, are conventionally modeled as *discrete* direct and cross-coupled linear spring and damping forces acting at the bearing center. However, the ratio of the bearing width to the shaft length in micro bearing-spindles is significant when compared to that in general rotordynamic systems. In addition the spindle shaft is more likely flexible. Therefore the HGJB in micro bearing spindles would rather function as a continuous support providing *distributed* restoring and damping forces.

Taking hard disk spindles as an example, the reasons that the model of distributed bearing forces is critical can be elaborated as follows. For disk drives with small form factors (e.g., 0.85-in HDD to be used in cell phones), most of the shaft surface is the bearings. In addition, most HDD spindles now use asymmetric herringbone grooved bearings, i.e., the two sides of the herringbone are not equal in length. The purpose of asymmetric herringbones is to prevent the fluid leakage. The net pumping force for the asymmetric bearing is in the direction to enforce the lubricant to stay in the reservoir. For asymmetric herringbone grooved bearing, it is more accurate to model the bearing as distributed load. Finally the bearing locations are very important for optimizing vibration performance of HDD spindles. With the distributed load model of the journal bearings, vibration performance of HDD can be better optimized.

To accurately predict dynamics and vibration of such micro bearing spindle systems, the research is to propose a new dynamic model of bearing forces provided by the journal bearing. In this research, herringbone grooved journal bearings (HGJB) for HDD are focused. The HGJB is modeled as a continuous support, providing the *distributed* restoring and damping forces. Furthermore a dynamical model of disk-spindle systems for HDD with distributed HGJB forces is developed for accurately predicting vibration in hard disk drives (HDD). Vibration analysis of the micro bearing spindle systems considering the distributed bearing forces should be useful for micro spindle design for various applications.

In summary this research work will effectively utilize an inter-disciplinary of two different fieldslubrication and complicated dynamics of micro disk-spindles--for accurately predicting vibration of micro spindle systems.

#### 2) Objectives

The main objective of this research is to develop a new dynamic model of disk-spindle systems with distributed HGJB forces for accurately predicting the vibration in hard disk drives. To accomplish this goal, the sub-tasks are defined subsequently as follows.

- 1. Determination of the distribution functions of bearing coefficients that characterize the distributed dynamic forces of the HGJB
- 2. Development of a dynamical model of disk-spindles systems with distributed dynamic forces in journal bearings for predicting vibration characteristics in micro spindle drives
- 3. Investigation of how the spindle model with distributed bearing forces improves the vibration prediction of the HDD through comparing the proposed model to the conventional model with discrete bearing forces

#### 3) Research methodology

- Phase I: Literature review; Problem statement; and Research plan (3 months)
- Phase II: Preliminary study: Modeling dynamic bearing forces as simple *uniform loads* and use this model for vibration prediction of HDD. The prelim simulation results show that the model with distributed bearing forces predicts the same natural frequencies but different modal damping of rocking modes, when compared to the prediction from the conventional discrete model. The difference in damping characteristics is more significant when the ratio of the bearing width and the shaft length is larger. (2 months)
- Phase III: Development of a dynamic model of distributed forces in herringbone groove journal bearings (HGJB) and determination of a distribution function of force coefficients of the HGJB that characterize the distributed bearing forces, as described in the following steps:
  - a) Formulate the Reynold equation governing pressure distribution of the HGJB. To determine the distribution of force coefficients of the HGJB, the pressure perturbation arising from the dynamic perturbations of journal displacements and velocities is analyzed using a variational approach. (2 months)
  - b) Develop the finite element program using MatLab<sup>®</sup> to solve for the steady-state pressure field and the pressure perturbation generated in the HGJB. The program is verified with the existing published numerical data. (2 months)
  - c) Determine the distribution functions of stiffness and damping coefficients along the bearing length by integrating the pressure perturbation over a circumferential direction. With these distribution functions, the distribution of linear, direct and cross-coupled spring and damping forces generated by the HGJB can be formulated. (2 months)
- Phase IV: Development of a dynamical model of disk-spindle system with the distributed bearing forces obtained from phase III through the use of Lagrange's mechanics, for vibration prediction of HDD. (3 months)

Phase V: Free and forced vibration analysis of various spindle drive systems, and investigation of an improvement of vibration prediction in HDD with the model of distributed bearing forces when comparing the proposed model to the conventional model of discrete bearing forces (3 months)

#### 4) Outcome of this research

- Publications: One international journal paper and one international conference in two years as listed:
   T. Jintanawan, "Vibration of Hard Disk Drive Spindle Systems with Distributed Journal Bearing Forces," *Microsystem Technologies*, Vol. 12, pp. 208-218, 2006.
  - **T. Jintanawan**, "Effects of Distributed Bearing Forces and Bearing Locations on Rocking Vibration of FDB Spindle Systems," *ASME Information Storage and Processing Systems Conference*, 2005.
- 2. Intellectual exchange of academic research between Chulalongkorn University and hard disk drive industrial research.
- 3. A summary with meaningful results and discussion on vibration analysis of the HDD spindles considering the distributed bearing forces for different models of sample drives is reported. This research results would be useful for the bearing spindle design of new HDD.

#### Chapter 2

# Detail of Research Work (เนื้อหางานวิจัย)

#### 1) Introduction

Micro bearing-spindle systems, defined in this report as the miniature spindle systems such that the bearing length is significant when compared to the shaft length, are found in many applications such as hard disk drives (HDD), precision instruments, and dental instruments. For various micro spindles such as hard disk spindles, herringbone grooved journal bearings (HGJBs) are currently used to provide restoring and damping forces in the radial direction. The grooves in such journal bearings are designed to improve half-speed whirl stability. In conventional approach, the dynamic forces in the journal bearings, including HGJBs, are modeled as *discrete* linear spring and damping forces acting at the bearing center [1, 2, 3, 4, 5]. The discrete bearing forces are then characterized by stiffness and damping coefficients in both in-line and cross-coupled directions as illustrated in Figure 1. However, the ratio of the bearing width to the shaft length in micro bearing-spindles is significant when compared with that in general rotordynamic systems. In addition the spindle shaft is more accurately modeled as a flexible shaft than as a rigid shaft [6, 7]. Therefore the journal bearings in micro bearing-spindles would rather function as a continuous support providing *distributed* restoring and damping forces.

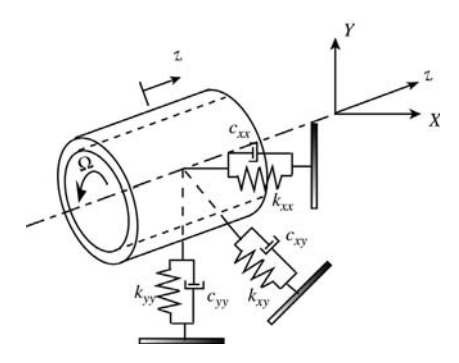


Figure 1: Conventional model of discrete forces in journal bearings

Taking hard disk spindles as an example, the reasons that the model of distributed bearing forces is critical can be elaborated as follows. For disk drives with small form factors (e.g., 0.85-in HDD to be used in cell phones), most of the shaft length is supported by the bearings. In addition, most HDD spindles now use asymmetric herringbone grooved bearings, i.e., the two sides of the herringbone are not equal in length. The purpose of asymmetric herringbones is to generate a net pumping force in the direction that enforces the lubricant to stay in the lubricant reservoir so that it will not leak out. With asymmetric herringbone grooved bearing, it is more accurate to model the bearing as distributed load. Finally the bearing locations are very important for optimizing vibration performance of HDD spindles [8, 9]. With modeling the journal bearings as distributed load, vibration performance of HDD can be better optimized.

To accurately predict dynamics and vibration of such micro bearing-spindle systems, a new dynamic model of bearing forces in the journal bearing is proposed. In this research, herringbone grooved journal bearings (HGJB) for HDD are focused. The HGJB is modeled as a continuous support, providing the axially distributed restoring and damping forces as shown in Figure 2. The research aims at determining the distribution functions of dynamic coefficients that characterize the distributed dynamic forces of the HGJB. First Reynolds equation governing a pressure field of the journal bearing is formulated. The pressure perturbation arising from the dynamic perturbations of journal displacements and velocities is then analyzed using a variational approach [2]. The finite element model (FEM) is developed to solve for the steady-state pressure field and the pressure perturbation generated in the HGJB. To determine the distribution functions of stiffness and damping coefficients along the bearing length, the pressure perturbation is integrated over a circumferential direction. With these distribution functions of stiffness and damping coefficients, the distributed linear spring and damping forces generated by the HGJB can be formulated. For the model validation, the total dynamic coefficients characterizing the discrete bearing forces of different HGJBs are compared with the values reported in various publications [3, 4]. The parameters of HGJB for HDD are used for the analysis. The steady-state pressure and the distribution functions of stiffness and damping coefficients of these HGJBs are presented. How the variation of parameters in HGJB affects the dynamic coefficients of the HGJB is also discussed.

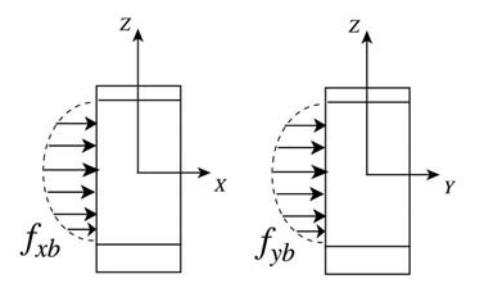
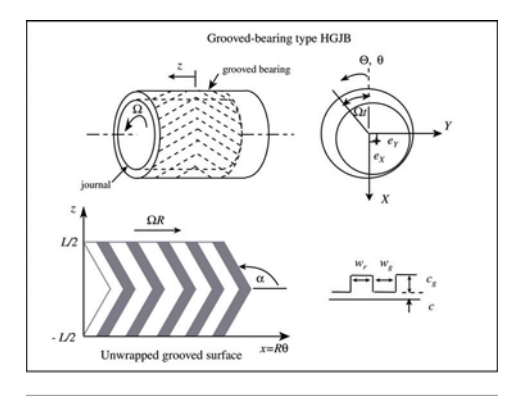


Figure 2: A model of distributed forces in journal bearings

The distributed dynamic model of the bearing forces in HGJB is further used in developing a mathematical model of the disk-spindle system for accurately predicting vibration in HDD. Free and forced transverse vibrations predicted by this present model are compared with those from the conventional spindle model with discrete bearing forces. How the distribution of bearing forces affects the vibration of HDD spindles is analyzed for various bearing widths.

#### 2) Dynamic model of distributed forces in herringbone groove journal bearings (HGJB)



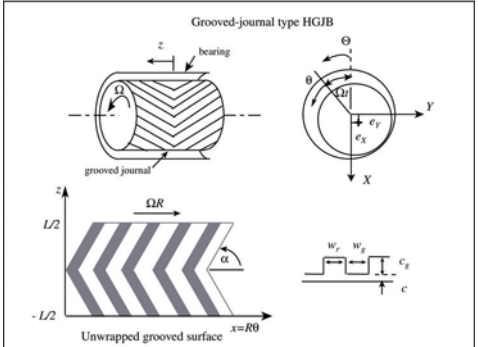


Figure 3: A herringbone groove journal bearing: grooved bearing type; and grooved journal type

Consider an arbitrary herringbone grooved journal bearing (HGJB) whose geometries are shown in Figure 3. The herringbones are symmetry and the bearing width is L. The journal has a radius R and rotates at a constant angular speed  $\Omega$ . For the spindles in hard disk drives, there exist two types of HGJB depending on the location of their grooves: a) the grooved-bearing (GB) type, and b) the grooved-journal (GJ) type, as shown in Fig. 3. The GB type has grooves located on the bearing sleeve, while the GJ type has grooves located on the rotating journal. The groove angles for both types are in the opposite direction, in order to pump the fluid inward. In Fig. 3, the inertial coordinate system XY is used to describe the motion of the journal center. The coordinate system xz, where  $x=R\theta$ , is used to describe the position of the unwrapped fluid film. With the grooves moving, the x-axis for the GJ type bearing is fixed to the rotating journal. In addition it is easier to consider the journal of the GJ-type bearing as relatively stationary while the bearing sleeve rotates in the opposite direction [3]. For the laminar flow of incompressible fluid film with negligible inertia and cavitation effects, the Reynolds equation governing the pressure field P in HGJB is

$$\frac{1}{R^{2}} \frac{\partial}{\partial \theta} \left( \frac{h^{3}}{12\mu} \frac{\partial P}{\partial \theta} \right) + \frac{\partial}{\partial z} \left( \frac{h^{3}}{12\mu} \frac{\partial P}{\partial z} \right) = L(P) = \frac{\Omega}{2} \frac{dh}{d\theta} + \frac{\partial h}{\partial t}, \text{ for GB type}$$

$$= -\frac{\Omega}{2} \frac{dh}{d\theta} + \frac{\partial h}{\partial t}, \text{ for GJ type}$$
(1)

where  $\mu$  is the fluid viscosity and h is the film thickness in the ridge and groove regions expressed respectively as

$$h = c + e_X \cos\Theta + e_Y \sin\Theta \tag{2}$$

and

$$h = c + c_g + e_X \cos \Theta + e_Y \sin \Theta \tag{3}$$

In (2) and (3),  $\Theta = \theta$  for the GB-type HGJB and  $\Theta = \theta + \Omega t$  for the GJ-type HGJB. The pressure field *P* must satisfy the following boundary conditions.

$$P(\theta, z, t) = P(\theta + 2\pi, z, t) \quad \text{and} \quad P(\theta, L/2, z) = P(\theta, -L/2, z) = P_a \tag{4}$$

where  $P_a$  is the atmospheric pressure.

For a small perturbation  $\Delta e_{\sigma}(t)$ ,  $(\sigma = X, Y)$ , of journal displacements from the steady state configuration  $(e_{X0}, e_{Y0})$ , the film thickness is then

$$h = h_0 + \Delta e_X \cos\Theta + \Delta e_Y \sin\Theta = h_0 + \sum_{\sigma} \Delta e_{\sigma} h_{\sigma}; \quad \sigma = X, Y$$
 (5)

where  $h_{\theta}$  is the film thickness for the steady state configuration  $(e_{X0}, e_{Y0})$ ,  $h_X = \cos \Theta$ , and  $h_Y = \sin \Theta$ . With the small perturbed displacement  $\Delta e_{\sigma}(t)$  and perturbed velocity  $\Delta \dot{e}_{\sigma}(t)$ ,  $(\sigma = X, Y)$ , the perturbed pressure field is then

$$P = P_0 + \sum_{\sigma} P_{\sigma} \Delta e_{\sigma} + \sum_{\dot{\sigma}} P_{\dot{\sigma}} \Delta \dot{e}_{\sigma}; \quad \sigma = X, Y$$
 (6)

where  $P_{\sigma}$  and  $P_{\dot{\sigma}}$  ( $\sigma = X$ , Y) are pressure perturbation with respect to the perturbed displacement and velocity, respectively. Substituting (5) and (6) into (1) and neglecting the higher order terms, the differential equation governing the steady-state pressure field is obtained as

$$L(P_0) = \frac{\Omega}{2} \frac{dh_0}{d\theta}, \text{ for GB type}$$

$$= -\frac{\Omega}{2} \frac{dh_0}{d\theta} - \Omega [e_{\chi_0} \sin \Theta - e_{\chi_0} \cos \Theta], \text{ for GJ type}$$
(7)

Moreover, for both GB- and GJ-types, the equations governing the pressure perturbation are then

$$L(P_{\sigma}) = \frac{\Omega}{2} \frac{dh_{\sigma}}{d\theta} - \frac{1}{R^2} \frac{\partial}{\partial \theta} \left( \frac{3h_0^2 h_{\sigma}}{12\mu} \frac{\partial P_0}{\partial \theta} \right) - \frac{\partial}{\partial z} \left( \frac{3h_0^2 h_{\sigma}}{12\mu} \frac{\partial P_0}{\partial z} \right); \quad \sigma = X, Y$$

$$L(P_{\sigma}) = h_{\sigma}; \quad \sigma = X, Y$$
(8)

Due to the discontinuity of the geometry from groove to ridge in the HGJB, finite element method (FEM) [3, 4] is used to discretize and solve (7) and (8) subsequently in order to determine the steady-state pressure field  $P_0$  and the pressure perturbation  $P_X$ ,  $P_Y$ ,  $P_{\dot{X}}$  and  $P_{\dot{Y}}$ .

To determine the distribution of stiffness and damping coefficients along the bearing length, the pressure perturbation is integrated over the circumferential direction. The distribution of stiffness and damping, being function of the bearing position z that measured from the bearing center along its length, are represented in a matrix form as

$$\mathbf{k} = \begin{bmatrix} k_{XX}(z) & k_{XY}(z) \\ k_{YX}(z) & k_{YY}(z) \end{bmatrix} = \int_{\theta} (-\cos\theta) \left[ P_X(z) & P_Y(z) \right] R d\theta$$
 (9)

and

$$\mathbf{c} = \begin{bmatrix} c_{XX}(z) & c_{XY}(z) \\ c_{YX}(z) & c_{YY}(z) \end{bmatrix} = \int_{0}^{\infty} (-\cos\theta) \left[ P_{\dot{X}}(z) & P_{\dot{Y}}(z) \right] R d\theta$$
 (10)

where  $k_{XX}(z)$  and  $k_{YY}(z)$  denote the direct stiffness distributions,  $k_{XY}(z)$  and  $k_{YX}(z)$  denote the cross-coupled stiffness distributions,  $c_{XX}(z)$  and  $c_{YY}(z)$  denote the direct damping distributions, and  $c_{XY}(z)$  and  $c_{YX}(z)$  denote the cross-coupled damping distributions. The distributions of stiffness and damping coefficients in (9) and (10) have units of N/m<sup>2</sup> and Ns/m<sup>2</sup>, respectively, characterizing the distributed bearing forces. Note that total stiffness and damping coefficients for the discrete bearing forces can be determined from an integration of  $k_{XX}(z)$ ,  $k_{XY}(z)$ ,  $c_{XX}(z)$ , and  $c_{XY}(z)$  over z. With the distribution functions of the bearing coefficients obtained from (9) and (10), the distributed restoring and damping forces per unit length provided by HGJB are

$$\begin{pmatrix} f_X(z,t) \\ f_Y(z,t) \end{pmatrix} = - \begin{bmatrix} k_{XX}(z) & k_{XY}(z) \\ k_{YX}(z) & k_{YY}(z) \end{bmatrix} \begin{pmatrix} r_X \\ r_Y \end{pmatrix} - \begin{bmatrix} c_{XX}(z) & c_{XY}(z) \\ c_{YX}(z) & c_{YY}(z) \end{bmatrix} \begin{pmatrix} \dot{r}_X \\ \dot{r}_Y \end{pmatrix}$$
(11)

where  $r_X(z, t)$ ,  $r_Y(z, t)$ ,  $\dot{r}_X(z, t)$ , and  $\dot{r}_Y(z, t)$  are infinitesimal displacement and velocity of the bearing, respectively. For the flexible rotor, the displacement and velocity depend on both longitudinal position z of the bearing and time t.

A finite element model (FEM) is developed to determine the distribution functions of stiffness and damping coefficients for HGJB. The model is validated by comparing the *total* dynamic coefficients for the discrete forces of two different HGJBs A and B with the values published in [3] and [4]. Table 1 lists the property and geometry of both bearings A and B, and the results are compared in Tables 2. It is shown that the compared results for both bearings match very well.

Table 1: Geometry and Property of bearing A and B

	Bearing A [4]	Bearing B [3]
Туре	GB	GJ
μ (Pa·s)	0.036	0.01
c (μm)	6	10
$\Omega$ (rpm)	7200	1500
R (mm)	2.006	10
α(°)	160	60
$c_g / c$	1	1
$w_r/(w_r+w_g)$	0.5	0.5
$N_g$	8	5
L/D	0.75	1
$e_0/c$	0	0

Table 2: Comparison of the total dynamic coefficients of bearing A and B

Dimensionless	Bearing A		
coefficients	Published model [4]	Present model	
$K^*_{XX}$	0.25	0.27	
$K*_{XY}$	0.55	0.62	
$C^*_{XX}$	1.25	1.35	
Coefficients	Bearing B		
Coefficients	Published model [3]	Present model	
$K_{XX}$ (N/m)	$2.4 \times 10^6$	$2.4 \times 10^{6}$	
$K_{XY}$ (N/m)	$3.75 \times 10^6$	$3.6 \times 10^6$	
$C_{XX}$ (Ns/m)	9×10 <sup>3</sup>	9.1×10 <sup>3</sup>	

[Note:  $K^*_{mn} = c \cdot K_{mn} / W^*$  and  $C^*_{mn} = c \cdot \Omega \cdot C_{mn} / W^*$ , where m, n = X, Y, and  $W^* = \mu \Omega LD(R/c)^2$ ]

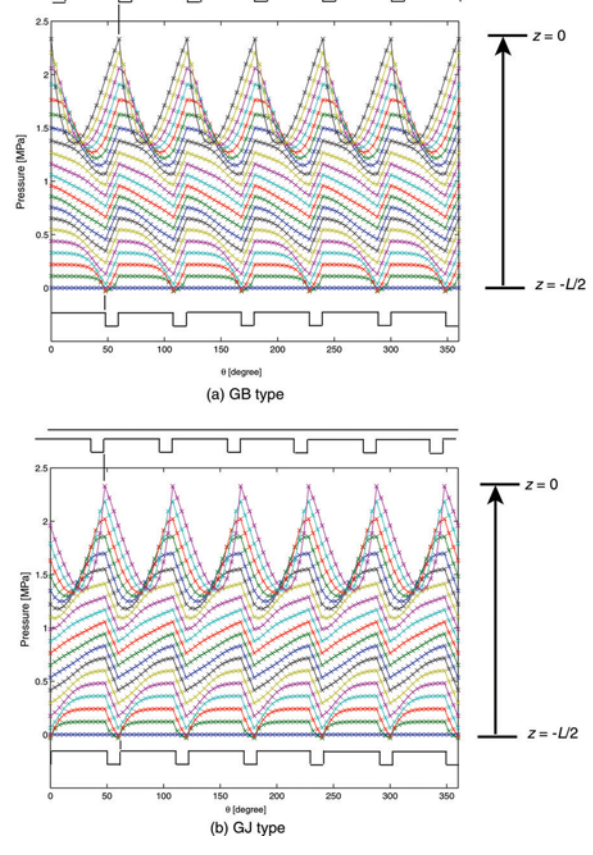
In the following subsections, both the GB- and GJ-type HGJBs for a hard disk drive are used for the analysis. The property and geometry of these HGJBs are listed in Table 3. In addition, the herringbones in these bearings are symmetric, i.e., two sides of the herringbones are equal in length. The steady-state pressure and the distributions of direct and cross-coupled stiffness and damping for both types of the HGJB are presented. The effects of parameter variation on the dynamic coefficients of the HGJB are investigated and discussed.

Table 3: Geometry and Property of the HGJB for HDD

μ (Pa·s)	0.0142
c (μm)	2.5
$\Omega$ (rpm)	7200
R (mm)	2
α(°)	23° (for GJ), 157° (for GB)
$c_g / c$	2.4
$w_r / w_r + w_g$	0.8
$N_g$	6
L/D	0.7
$e_0/c$	0

#### 2.1. Steady-State Pressure

Figure 4 illustrates the steady-state pressure field generated in the HGJBs. Each curve represents the pressure distribution along the circumference at a certain location z along the longitudinal axis. The circumferential pressure distributions from the end of the bearing (z = -L/2) to the middle of the bearing (z = 0) are shown in the figure. Due to the symmetry of the groove pattern, the pressure distribution for the other half ( $0 \le z \le L/2$ ) is identical to that presented in Fig.4. Comparing the pressure profiles at different longitudinal position z, the pressure builds up from the atmospheric pressure at both ends (z = -L/2, and z = L/2) and reaches the maximum at the middle of the bearing (z = 0). It is interesting to note that the pressure slightly drops below the atmospheric pressure in the region close to the both ends of the bearing ( $z \approx \pm L/2$ ) at the ridge to groove for the GB type (at the groove to ridge for the GJ type). This negative pressure causes the fluid to be pumped inward around this region. Hence the abrupt change of the geometry in HGJB would help reduce the fluid leakage. Moreover, the pressure is a repetitive function of the bearing angle  $\theta$ , as shown in Fig.4. A cycle of the repetition corresponds to the width of each groove and ridge. At the middle of the bearing (z = 0), the pressure reaches the maximum at the abrupt change of the geometry from ridge to groove for the GB type, and from groove to ridge for the GJ type. With such pressure distribution in HGJB, the fluid is pumped inward along the grooves.



7.

Figure 4: Steady-state pressure field

#### 2.2. Distribution of dynamic coefficients

Figures 5 and 6 show the distribution functions of dynamic coefficients for GB- and GJ-types HGJB, respectively, along various longitudinal position z. The theoretical simulation yields  $k_{XX}(z) = k_{YY}(z)$ ,  $k_{XY}(z) = -k_{YX}(z)$ ,  $c_{XX}(z) = c_{YY}(z)$ , and  $c_{XY}(z) = -c_{YX}(z)$ . This so-called isotropic property occurs in the lightly loaded bearing such as the HGJB for hard disk drives. For both types of HGJB in Figs. 5 and 6, the distributions of direct and cross-coupled stiffness and the distribution of direct damping gradually increase from both sided-ends of the bearing, and reach the maximum at the bearing center. The variation of these coefficients along the bearing length indicates that the distributed bearing forces are not uniform. Specifically, the HGJB functions as stiffer springs and larger dampers at the bearing center than at both ends. In addition the cross-coupled stiffness  $k_{XY}(z)$  is larger than the direct stiffness  $k_{XX}(z)$  for both cases. For a comparison, Figure 7 shows the distribution of force coefficients of the plain journal bearing with identical geometry. Comparing Figs. 5 and 6 to Fig. 7, the HGJB possesses nonzero direct stiffness, resulting in the in-line forces to cancel out the destabilizing cross-coupled forces. Hence the HGJB helps stabilize the spindle at half-speed whirl. Finally the total dynamic coefficients for both types of the HGJB and for the plain journal bearing are listed in Table 4. Note that the cross-coupled damping coefficients for all cases are zero.

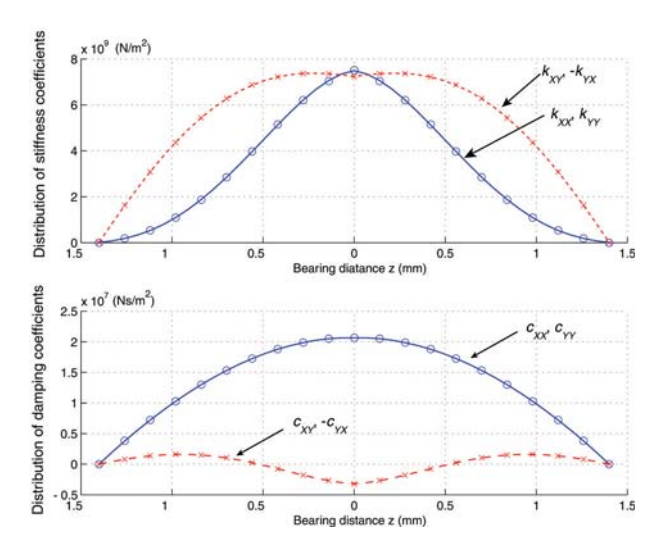


Figure 5: Distributions of dynamic coefficients of the GB-type HGJB

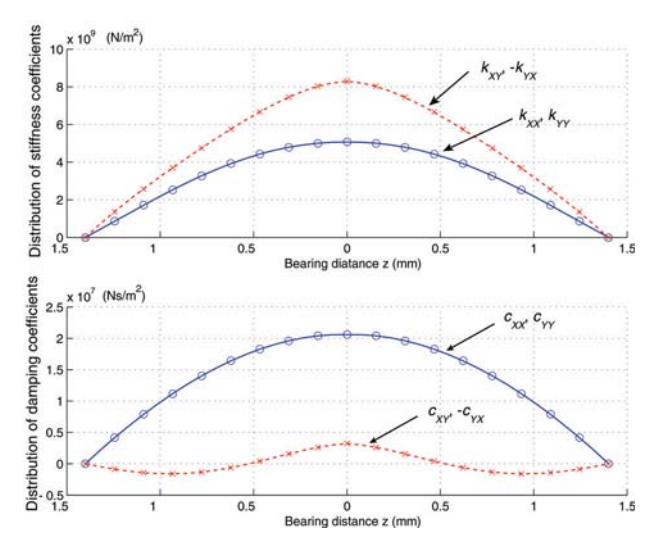


Figure 6: Distributions of dynamic coefficients of the GJ-type HGJB

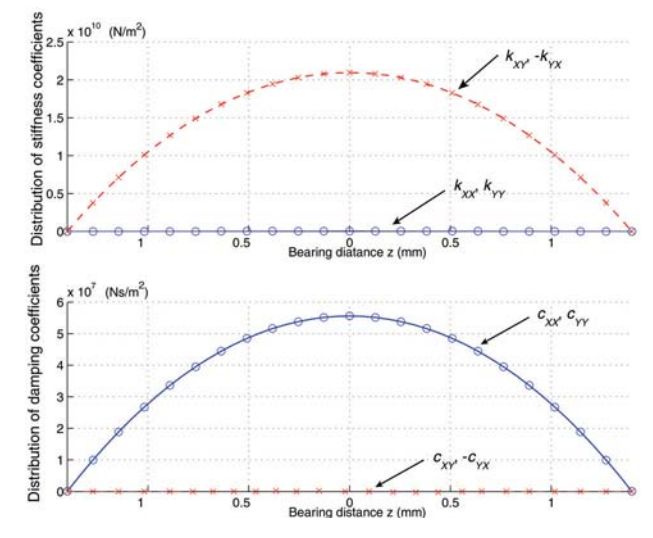


Figure 7: Distributions of dynamic coefficients of the plain journal bearing

Coefficients	GB type	GJ type	Plain JB
$K_{XX}$ (N/m)	9.1615×10 <sup>6</sup>	9.1243×10 <sup>6</sup>	0
$K_{XY}$ (N/m)	1.4964×10 <sup>7</sup>	1.3964×10 <sup>7</sup>	$3.9415 \times 10^7$
$C_{XX}$ (Ns/m)	$3.8352\times10^{4}$	3.8352×10 <sup>4</sup>	1.0451×10 <sup>5</sup>

0

0

Table 4: Total dynamic coefficients of the HGJB and the plain journal bearing

0

 $C_{XY}$  (Ns/m)

The effect of parameter variation on the dynamic coefficients of HGJB is then investigated. Figures 8 to 12 show the distributions of dynamic coefficients for the GB-type bearing when varying each parameter such as: rotating speed, viscosity, bearing width, groove angle, and groove depth, respectively. In addition the total coefficients of each case are summarized in Table 5. The cross-coupled dampings are zero and the results are omitted here. When each parameter is varied, the distribution shapes of dynamic coefficients in Figs. 8-12 remain unchanged. Nevertheless the values of these coefficients depend on each parameter as discussed next.

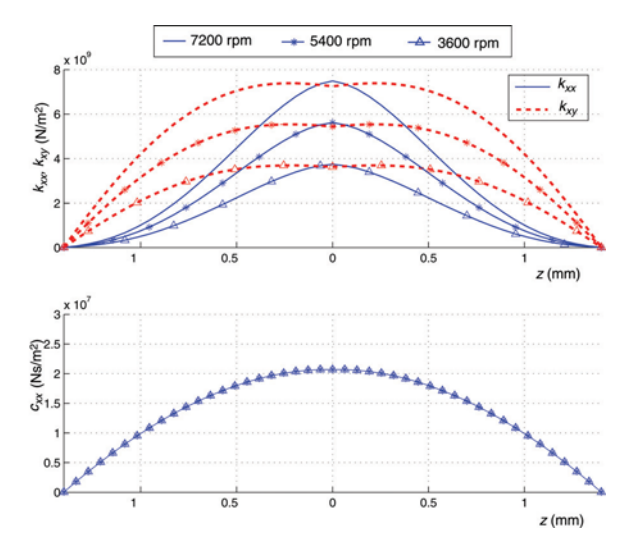


Figure 8: Distributions of dynamic coefficients of the GB-type HGJB for various speeds

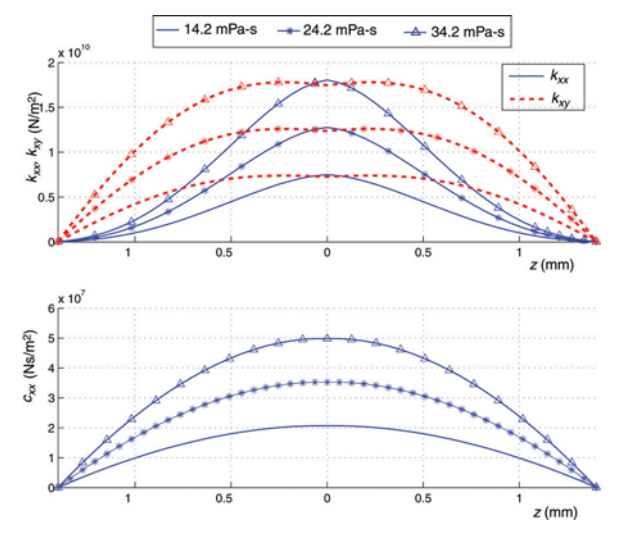


Figure 9: Distributions of dynamic coefficients of the GB-type HGJB for various viscosities

In Fig. 8, an increase in the rotating speed results in higher direct and cross-coupled stiffness but has no effect on the damping. Both the direct and cross-coupled stiffness coefficients are linearly proportional to the rotating speed, as seen in Table 5. In Fig. 9, the direct and cross-coupled stiffness coefficients and the direct damping coefficient linearly increase as the viscosity increases. Furthermore with larger bearing width, all dynamic coefficients are higher as seen in Fig. 10. It is because the wider bearing yields larger area to generate the pressure. In Fig. 11, as the groove angle decreases from  $157^{\circ}$  to  $120^{\circ}$ , the direct stiffness  $k_{XX}(z)$  significantly decreases. The cross-coupled stiffness  $k_{XY}(z)$  and the direct damping  $c_{XX}(z)$  in Fig. 11 also decrease when the angle changes from  $157^{\circ}$  to  $140^{\circ}$ . However there is no significant change of  $k_{XY}(z)$  and  $c_{XX}(z)$  when the angle increases from  $140^{\circ}$  to  $120^{\circ}$ . Therefore the groove angle has significant effects on the direct stiffness. With steep angle, the area of grooves for pumping pressure is reduced, resulting in lower direct stiffness coefficient. Finally the larger groove depth yields lower cross-coupled stiffness and direct damping, but has no significant effect on the direct stiffness, as shown in Fig. 12. This can be explained by the less effective pumping action in the bearing as the groove depth becomes larger.

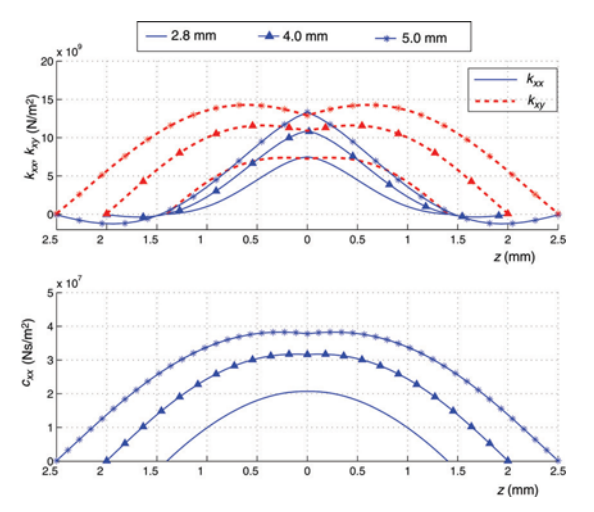


Figure 10: Distributions of dynamic coefficients of the GB-type HGJB for various bearing widths

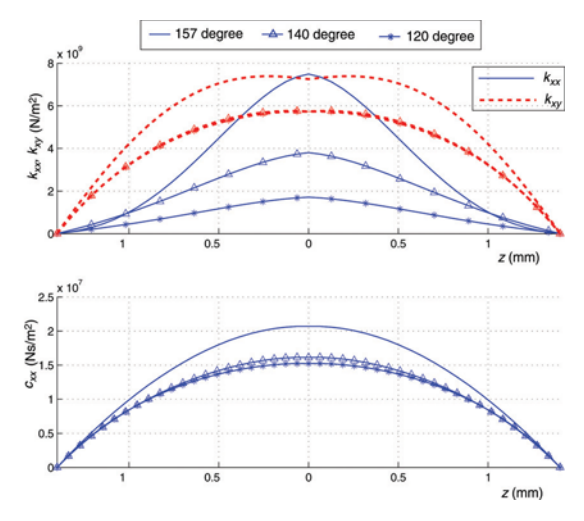


Figure 11: Distributions of dynamic coefficients of the GB-type HGJB for various groove angles

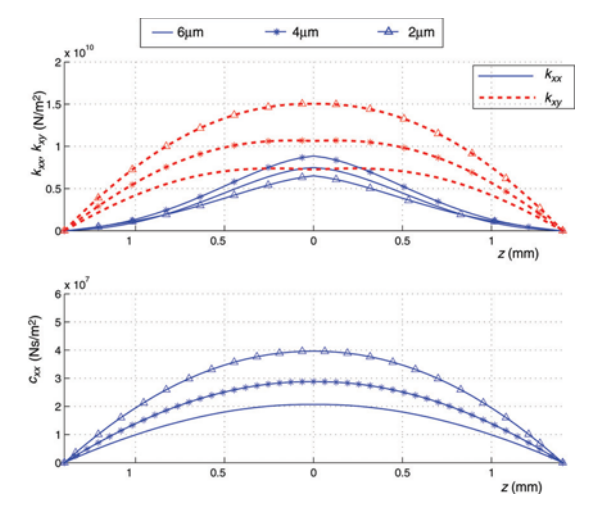


Figure 12: Distributions of dynamic coefficients of the GB-type HGJB for various groove depths

Table 5: Total dynamic coefficients of the GB-type HGJB with varied parameters

Speed (rpm)	$K_{XX}$ (N/m)	$K_{XY}$ (N/m)	$C_{XX}$ (Ns/m)
7200	$9.1385 \times 10^6$	1.4937×10 <sup>7</sup>	3.8241×10 <sup>4</sup>
5400	6.8712×10 <sup>6</sup>	1.1223×10 <sup>7</sup>	3.8352×10 <sup>4</sup>
3600	$4.5808 \times 10^6$	$7.4820 \times 10^6$	$3.8352\times10^{4}$
Viscosity (mPa-s)	$K_{XX}$ (N/m)	$K_{XY}$ (N/m)	$C_{XX}$ (Ns/m)
14.2	9.1385×10 <sup>6</sup>	1.4937×10 <sup>7</sup>	3.8241×10 <sup>4</sup>
24.2	1.5613×10 <sup>7</sup>	$2.5502 \times 10^7$	6.5360×10 <sup>4</sup>
34.2	$2.2065 \times 10^7$	$3.6040 \times 10^7$	9.2369×10 <sup>4</sup>
Bearing length (mm)	$K_{XX}$ (N/m)	$K_{XY}$ (N/m)	$C_{XX}$ (Ns/m)
28	$9.1385 \times 10^6$	1.4937×10 <sup>7</sup>	3.8241×10 <sup>4</sup>
40	1.4435×10 <sup>7</sup>	$3.3464 \times 10^7$	8.5634×10 <sup>4</sup>
50	1.7434×10 <sup>7</sup>	5.1071×10 <sup>7</sup>	1.3126×10 <sup>5</sup>
Groove angle (°)	$K_{XX}$ (N/m)	$K_{XY}$ (N/m)	$C_{XX}$ (Ns/m)
157	$9.1385 \times 10^6$	1.4937×10 <sup>7</sup>	3.8241×10 <sup>4</sup>
140	5.4568×10 <sup>6</sup>	1.1452×10 <sup>7</sup>	$3.0841 \times 10^4$
120	2.4617×10 <sup>6</sup>	1.1345×10 <sup>7</sup>	2.9865×10 <sup>4</sup>
Groove depth (μm)	$K_{XX}$ (N/m)	$K_{XY}$ (N/m)	$C_{XX}$ (Ns/m)
6	9.1385×10 <sup>6</sup>	1.4937×10 <sup>7</sup>	3.8241×10 <sup>4</sup>
4	1.0967×10 <sup>7</sup>	2.0962×10 <sup>7</sup>	5.3530×10 <sup>4</sup>
2	8.1778×10 <sup>6</sup>	2.8456×10 <sup>7</sup>	7.4138×10 <sup>4</sup>

#### 3) Mathematical model of hard disk drive spindle system with distributed bearing forces

The mathematical model of fluid dynamic bearing (FDB) spindle systems with distributed journal bearing forces, for predicting the *transverse* vibration of a HDD, is developed. The equations governing the transverse

motion of the spindle systems are derived using Lagrange's method. Most detailed derivation is not different from that presented in [6] and would be omitted here. This report however focuses on a formulation of the distributed bearing forces provided by HGJB and a contribution of these distributed forces to the dynamical model of the system, which were presented in Section 2.

Figure 13 shows a physical model of the FDB spindle system in HDD. The system consists of N elastic circular disks clamped to a deformable hub that allows infinitesimal rigid-body translation and rocking. The hub is press-fit onto a *rotating, flexible* shaft, which is mounted to the base through two herringbone-grooved journal bearings (HGJB) and a spiral-grooved thrust bearing. The HGJBs provide *distributed* direct and cross-coupled spring and damping forces in the radial direction. The thrust bearing provides the axial restoring and damping forces against the spindle axial motion as well as the restoring- and damping-rocking moments against the spindle rocking. In order to provide the rocking moment to the system, the thrust bearing is modeled as torsional springs and dampers through the angular direct and cross-coupled stiffness and damping coefficients,  $k_{r1}$ ,  $k_{r2}$ ,  $c_{r1}$ ,  $c_{r2}$  [6]. According to large deformation of the hub around the press-fit, the hub-shaft interface is modeled as a hinged support with a torsional spring. In this model, the spindle system is axisymmetric and all the disks are identical. Only the zero-nodal-circle modes of the disk vibration are retained in the mathematical model because of their significance in the frequency range of interest. Moreover the motion of the system in the spindle's transverse and axial directions can be completely decoupled [6]. In this study, the spindle spins at a constant speed  $\omega_3$  and is subjected to the base excitation in the disk-plane direction, thus the system exhibits only the transverse motion.

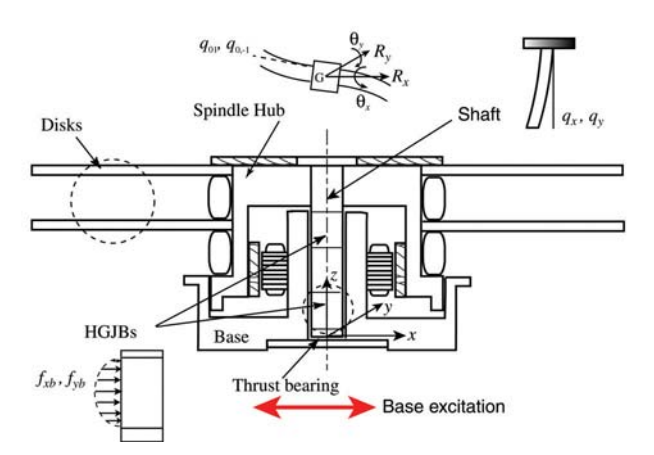


Figure 13: A FDB spindle system for HDD

The transverse motion of the FDB spindle system for HDD is described by the following generalized coordinates: infinitesimal rigid body whirling of the spindle hub; infinitesimal rigid body precession of the hub; eigenmodes of the flexible shaft; and the (0,1) eigenmodes of each disk. The mathematical model governing the transverse motion of the FDB spindle system for HDD is published in detail by the author in [10], and this journal paper is attached in the appendix.

#### 4) Vibration analysis

In this section, free and forced vibrations of the hard disk drive spindle systems with distributed bearing forces are analyzed for various aspect ratios of the bearing width to the shaft length. For the free vibration, natural

frequencies and modal dampings of the transverse modes are present. The modal damping indicates the shape of resonance peak and characteristics of the resonance amplitudes when subjected to the excitation. For forced vibration, transverse frequency response functions (FRF) of the system subjected to the base excitation in the disk-plane direction are present. Free and forced vibrations predicted by the model in Section 3 are compared to those predicted by the conventional model with discrete bearing forces [6]. Effect of the distributed bearing forces of HGJBs on the natural frequencies, modal dampings and transverse FRF of the spindle system is then discussed.

Two nearly identical disk-spindle systems A and B for HDD, with only difference in bearing width, are studied. Both systems have two-disk platter. Geometries and properties of the disks and spindle are listed in [10]. Each spindle consists of two identical HGJB whose property and geometry, except L/D, are previously shown in Table 3. In addition the bearing width of spindles A and B are 2.8 and 5 mm, respectively. Thus the aspect ratios of each bearing width to the shaft length for both spindles are 0.17 and 0.30, respectively. The angular stiffness and damping coefficients of the thrust bearing are assumed small and negligible in this case.

#### 4.1. Free Vibration

The model of spindle system with distributed bearing forces developed in Section 2.3 predicts the natural frequencies and the modal dampings of spindles A and B as illustrated by the solid lines in Fig. 14 for various spin speeds. In addition, these results are compared to the values predicted by the model with discrete bearing forces as shown by the dashed lines in the same plot. Furthermore the values of the natural frequencies and the modal dampings of spindles A and B for 120 Hz spin speed that predicted by both models are presented in Tables 6 and 7. Both spindle models with either discrete or distributed bearing forces predict similar characteristics of the transverse vibration which can be divided into two groups: a) four half-speed whirl (HSW) modes, and b) two pairs of rocking modes; see Fig. 14. Each modeshape exhibits a coupled motion of the spindle whirling and precession, the flexible shaft vibration and the disk vibration of (0,1) modes [6, 7, 8]. All these vibration modes exist in the transverse direction, and hence are the main cause of the track misregistration. In Fig. 14, the halfspeed whirls occur at a certain frequency about half of the rotor speed, and they are heavily damped compared to the rocking modes. The frequencies and damping of the rocking mode pairs have two split branches known as backward (B) and forward (F) modes, as seen in Fig. 14. In addition, for both rocking mode pairs, the modal damping of the backward modes is always slightly greater than the damping of the forward modes as shown in Tables 6 and 7. In practice, the predictable half speed whirl can be corrected by the servo system in HDD. Therefore it is the rocking modes that are the major concern in optimizing the vibration performance of HDD spindles. Moreover only the spindle model considering the shaft and disk flexibility can predict these two rocking mode pairs.

Table 6: Natural frequencies and modal dampings of spindle A (bearing width = 2.8 mm)

Vibration	Natural frequencies (Hz)		Natural frequencies (Hz) Modal damping (%)		damping (%)
modes	Discrete model	Distributed model	Discrete model	Distributed model	
HSW	62.5	62.5	60	60	
Rocking B1	285	285	3.23	3.99	
Rocking F1	515	515	1.78	2.33	
Rocking B2	1893	1893	1.24	1.84	
Rocking F2	2089	2088	1.20	1.75	

Table 7: Natural frequencies and modal dampings of spindle B (bearing width = 5.0 mm)

Vibration	Natural frequencies (Hz)		cies (Hz) Modal damping (%)	
modes	Discrete model	Distributed model	Discrete model	Distributed model
HSW	62	62	34	32
Rocking B1	282	283	1.97	7.09
Rocking F1	513	514	1.29	5.01
Rocking B2	1902	1897	1.20	5.16
Rocking F2	2100	2094	1.15	4.78

Compared to the conventional model of discrete bearing forces, the spindle model with distributed bearing forces predicts the same natural frequencies for all transverse modes but predicts higher modal dampings of the rocking mode pairs. The difference in damping prediction is clearer for spindle *B* where the ratio of the bearing width to the shaft length becomes larger. It implies that under the base excitation, the resonance peaks of the rocking modes predicted by the model with distributed bearing forces are more heavily damped (the peaks are less steep) and the rocking amplitude is smaller when compared to those predicted by the conventional model of discrete bearing force. In the spindle design, the rocking amplitudes have to be minimized in order to optimize the vibration performance. With the higher modal damping of the rocking modes, the vibration performance of HDD spindles is better.

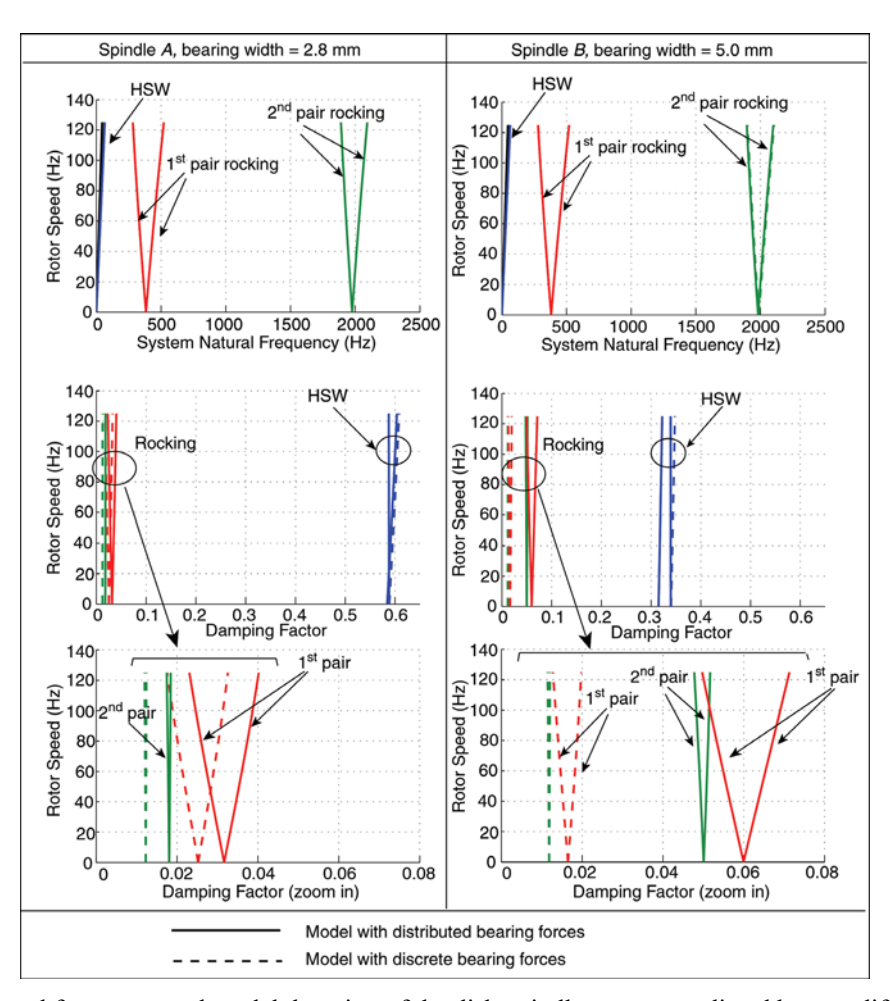


Figure 14: Natural frequency and modal damping of the disk-spindle system predicted by two different models: with distributed bearing forces and with discrete bearing forces, for the bearing width of 2.8 and 5.0 mm

The same predictions of natural frequency for both models can be explained as follows. The half speed whirls are an inherence whirl phenomena of the bearing and their resonance frequency is only affected by the spin speed. Furthermore the frequencies of the rocking mode pairs substantially depend on the natural frequencies of the shaft and disk. Accordingly the bearing property and geometry has no great effect on all resonance frequencies. The difference in damping predictions of the rocking modes from the two models can be discussed as follows. The modal damping of the rocking modes is mainly affected by the damping in the bearing as well as the bearing deflection. For the distributed bearing forces, the bearing deflection is considered as continuously varied along the bearing length due to the shaft flexibility. Thus it results in different values of modal dampings compared to those predicted by the spindle model with discrete bearing forces that the bearing deflection is simply evaluated at the bearing center.

To further investigate the effect of shaft flexibility on the modal damping that predicted by the model with distributed bearing forces, Fig. 15 compares the natural frequencies and modal dampings<sup>1</sup> of two different flexible-disk spindle systems: 1) with rigid shaft; and 2) with flexible shaft, for various spin speed. When compared to the flexible-shaft system, the system with rigid shaft possesses four half-speed whirl modes but

<sup>&</sup>lt;sup>1</sup> For all cases, the modal dampings of the half-speed whirl modes are not different, and hence they are not shown in Fig. 15.

only one pair of rocking modes. This is because of reduced degrees of freedom in the system. Moreover the modal dampings of rocking modes for the rigid-shaft spindle system, predicted by the models with either discrete or distributed bearing forces, are nearly identical, as seen on the left of Fig. 15. It is implied that the model of distributed bearing forces does not cause any difference in damping prediction unless the shaft is flexible. For the rigid shaft, the deflection of the bearing, which is affected by only the whirling and the rocking of the rigid spindle, slightly varies along its length. In such case, the dynamic resultants of bearing forces obtained from either discrete or distributed models are not different, and hence resulting in similar vibration characteristics.

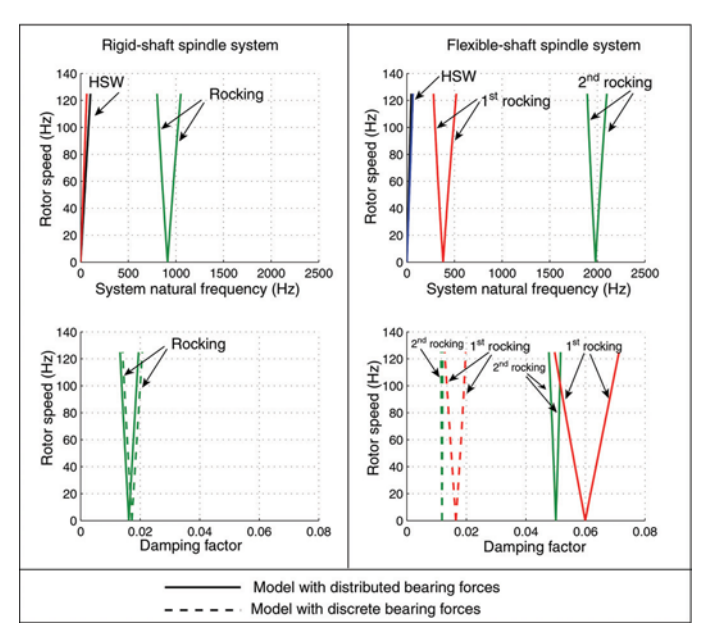


Figure 15: Free vibration prediction of the rigid-shaft and flexible-shaft spindle systems with the bearing width of 5.0 mm

For the FDB spindle system with significant aspect ratio of the bearing width to the shaft length and the shaft is likely flexible, the conventional spindle model with discrete bearing forces would not accurately predict the modal damping of rocking modes. In such system, the dynamic model of disk-spindle system with distributed bearing forces could be the alternative model for improving the damping prediction.

#### 4.2. Forced Vibration

In this section, we present a simulation of frequency response functions (FRF) whose response is measured from the disk along the radial or transverse direction, when subjected to the base excitation in the disk-plane direction. This transverse vibration consists of two components: one from the spindle whirling and the other from the spindle precession.

Figure 16 shows the magnitudes of transverse FRF of the previously described disk-spindle systems A and B, when the response is measured from the lower disk and the spindle spins at 7200 rpm or 120 Hz. In Fig. 16 the transverse FRF of both systems A and B that predicted by the spindle models with discrete and distributed bearing forces are compared. In all cases, for the frequency range of 0-800 Hz there exist the resonance peaks of half-speed whirl modes at 60 Hz and the first pair of backward and forward rocking modes at 270 and 520 Hz.

Moreover the resonance peaks of rocking modes predicted by the present model with distributed bearing forces are more heavily damped. The larger damping of rocking modes is much clearer for the case of system *B* with wider bearing width.

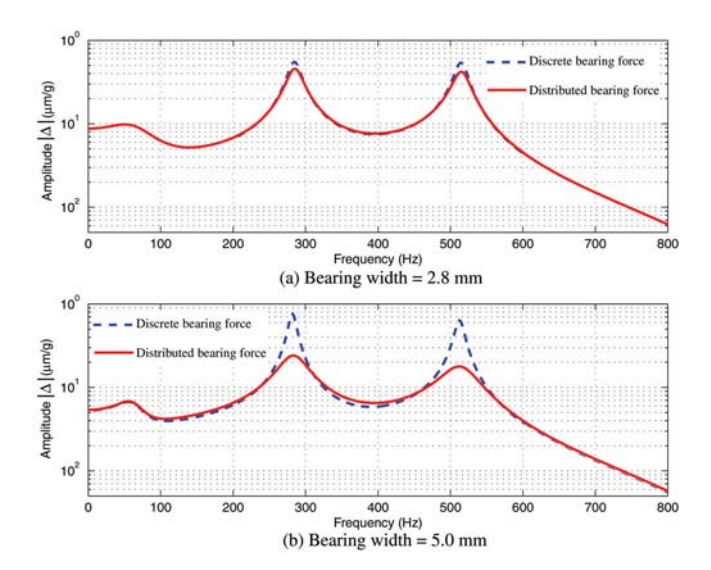


Figure 16: Transverse FRF of the disk-spindle system predicted by two different models: with distributed bearing forces and with discrete bearing forces, for the bearing width of 2.8 and 5.0 mm

#### 5) Conclusions

A new dynamic model of the distributed forces in a HGJB is proposed for micro bearing-spindle system in which the aspect ratio of the bearing width to the shaft length is significant, and the shaft is flexible. The distributed bearing forces are characterized by the distribution functions of direct and cross-coupled stiffness and damping coefficients. The model is validated by comparing the total dynamic coefficients with the published numerical values for various HGJBs. In the analysis, the actual parameters for HGJB in hard disk spindles are considered, and the distributions of the stiffness and damping coefficients are determined. The effects of the parameter variation on the dynamic bearing coefficients are then discussed. The model of distributed bearing forces in the HGJB is further applied to the dynamical model of disk-spindle systems for HDD for improving the accuracy of the vibration prediction. When compared to vibration predicted by the conventional spindle model of the disk-spindle system with discrete bearing forces, the present dynamical model with distributed bearing forces predicts the same natural frequencies for all transverse modes but higher modal damping of the rocking modes. The difference in damping prediction is clearer when the aspect ratio of the bearing width to the shaft length becomes larger and the shaft is likely flexible. Specifically, the modal damping of the rocking modes is substantially affected by the journal bearing forces. For the present model, these bearing forces are distributed along the bearing length where the bearing deflection is continuously varied due to the shaft flexibility. The spindle model with distributed bearing forces could be the alternative model for improving the damping prediction of the rocking modes.

#### 6) References

- 1. Hamrock BJ. Fundamentals of fluid film lubrication. McGraw-Hill, 1994.
- Klit P Lund JW. Calculation of the dynamic coefficients of a journal bearing using a variational approach.
   ASME Journal of Tribology 1988;108:421-425.
- 3. Zirkelback N San Andres L. Finite element analysis of herringbone groove journal bearings: a parametric study. ASME Journal of Tribology 1998;120:234-240.
- 4. Jang G Kim Y. Calculation of dynamic coefficients in hydrodynamic bearing considering five degree of freedom for a general rotor-bearing system. ASME Journal of Tribology 1999;121:499-505.
- Zang G Hatch MR. Analysis of coupled journal and trust hydrodynamic bearing using a finite-volume method. ASME Advances in Information Storage and Processing System 1995;1:71-79.
- Jintanawan T, Shen IY Tanaka K. Vibration Analysis of Fluid Dynamic Bearing Spindles with Rotating-Shaft Design. IEEE Transactions on Magnetics 2001;37:799-803.
- Jintanawan T, Ku C-PR Zhu J. Effects of Thrust Hydrodynamic Bearing Stiffness and Damping on Disk-Spindle Axial Vibration in Hard Disk Drives. Microsystem Technologies 2004;10:338-344.
- 8. Park JS, Shen IY Ku CP. A parametric study on rocking vibration of rotating disk/spindle systems with hydrodynamic bearings: rotating shaft design. Microsystem Technologies 2002;8:427-434.
- Jintanawan T. FDB spindle motor design for vibration suppression. Proceedings of the IEEE Asia-Pacific Magnetic Recording Conference, 2002.
- Jintanawan T. Vibration of Hard Disk Drive Spindle Systems with Distributed Journal Bearing Forces. Microsystem Technologies 2006; 12:208-218.

## Appendix

#### TECHNICAL PAPER

Thitima Jintanawan

# Vibration of hard disk drive spindle systems with distributed journal bearing forces

Received: 8 October 2004 / Accepted: 4 May 2005 / Published online: 18 October 2005 © Springer-Verlag 2005

**Abstract** This paper is to analyze vibration of fluid dynamic bearing spindles with distributed journal bearing forces. The dynamical model is developed to predict the transverse vibration of the disk-spindle systems in HDD where an aspect ratio of the bearing width to the shaft length is significant and the shaft is likely flexible. In such spindles the journal bearing functions as a continuous support, providing the distributed restoring and damping forces, and is therefore modeled as distributed linear spring and damping forces through distribution functions of dynamic coefficients. Vibration analysis reveals that the spindle model with distributed bearing forces predicts the same natural frequencies for all transverse modes but higher modal damping of the rocking modes, when compared to the values predicted by the conventional model with discrete bearing forces. The difference in damping prediction is clearer for the flexible-shaft spindle whose ratio of the bearing width to the shaft length becomes larger.

#### 1 Introduction

Fluid dynamic bearing (FDB) spindle motors are currently used in hard disk drive (HDD) because of the FDB capability in vibration and acoustic reduction. In the FDB spindle drives, the herringbone grooved journal bearings (HGJB) are used to provide restoring and damping forces in the radial direction. In conventional approach, the dynamic forces provided by the journal bearings, including HGJBs, are modeled as discrete linear spring and damping forces acting at the bearing center (Booser 1984; Klit et al. 1986; Zirkelback et al. 1998; Jang et al. 1999).

T. Jintanawan Department of Mechanical Engineering, Chulalongkorn University, Bangkok, Thailand 10330 E-mail: Thitima.j@chula.ac.th

The transverse vibration of HDD spindles, occurring in the disk-plane direction, is the main cause of the track misregistration that limits the storage density performance. It has been known that the property and location of HGJB play an important role in optimizing such unwanted transverse vibration (Park et al. 2002). To develop a dynamic model predicting the vibration of the disk-spindle systems for HDD, one can observe that geometry of the bearing-spindle in HDD is quite unique; i.e., the aspect ratio of the bearing width to the shaft length is *significant* or greater when compared with that in general rotordynamic systems. Taking disk drives with small form factors (e.g., 0.85 in. HDD to be used in cell phones) as an example, most of the shaft length is supported by the bearings. In this case the aspect ratio of the width for each bearing to the shaft length could be as great as 0.5. In addition the spindle shaft in HDD is more accurately modeled as a flexible shaft than a rigid shaft (Jintanawan et al. 2001). With these observations, the HGJBs in the HDD spindles would rather function as a continuous support providing distributed restoring and damping forces. Jintanawan (2004) proposes a new dynamic model of distributed bearing forces in HGJB. In the paper, the distribution functions of dynamic coefficients characterizing the distributed forces of the HGJB were determined.

This paper is to further develop a dynamical model of disk-spindle systems with distributed forces in HGJB for predicting vibration in HDD. The HGJB is modeled as distributed linear spring and damping forces through distribution functions of the direct and cross-coupled spring and damping coefficients. Determination of these coefficients is presented in Sect. 2. The mathematical model of disk-spindle systems with distributed bearing forces is then developed and summarized in Sect. 3. In Sect. 4, free and forced transverse vibrations predicted by this present model are compared with those from the conventional spindle model with discrete bearing forces. How the distribution of bearing forces affects the vibration of HDD spindles is analyzed for various bearing widths.

## 2 Determination of distribution of dynamic bearing coefficients

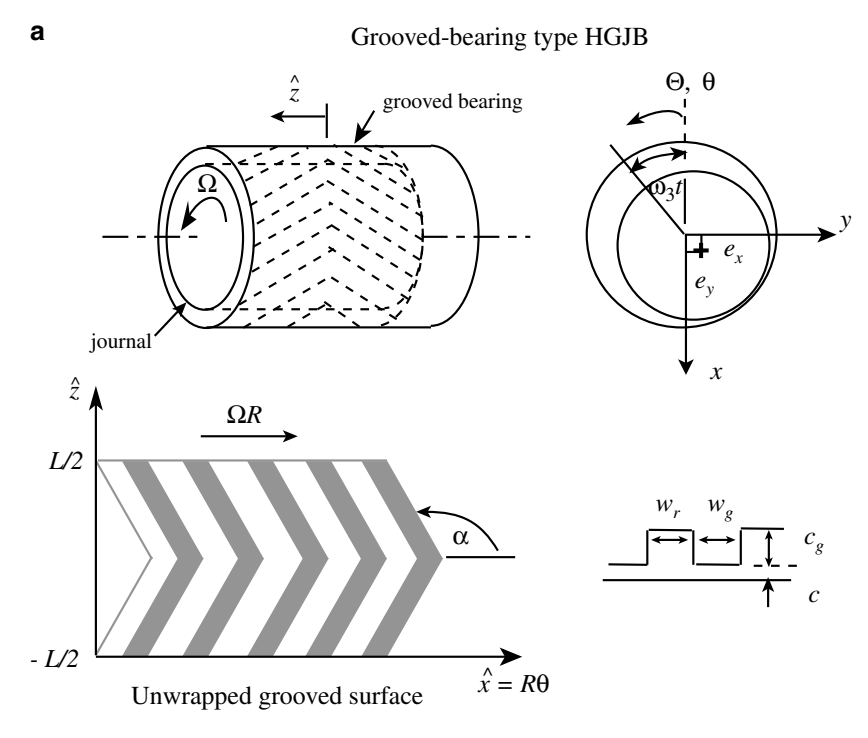
Consider an arbitrary HGJB as shown in Fig. 1. There exists two types of HGJB for HDD spindles depending on the location of their grooves: (a) the grooved-bearing (GB) type, and (b) the grooved-journal (GJ) type. The GB type has the grooves located on the bearing sleeve, while the GJ type has the grooves located on the rotating

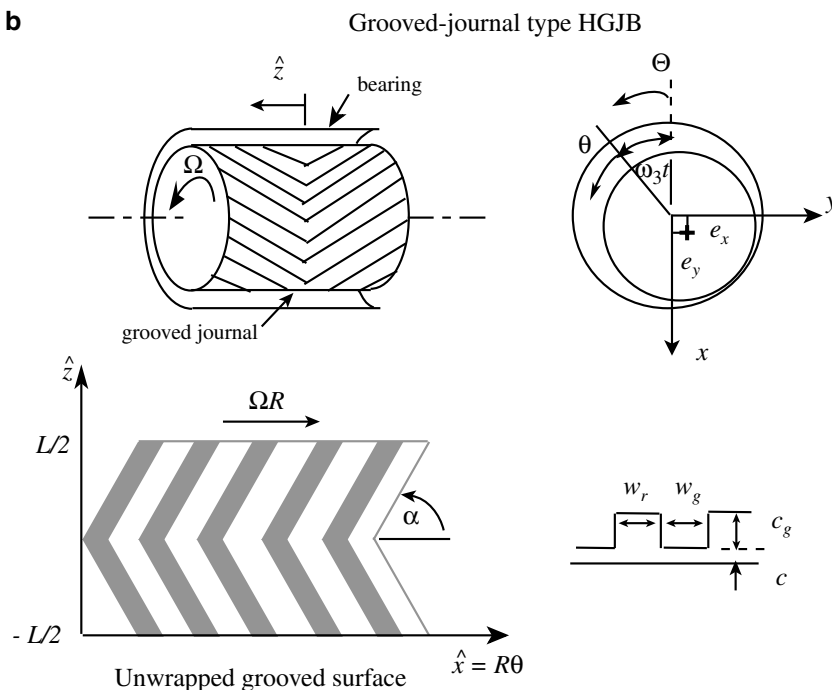
There radius rad

journal. The groove angles for both types are in the opposite direction, in order to pump the fluid inward. In addition, the bearing width is L and the journal having a radius R rotates with a constant angular speed  $\omega_3$ .

To determine the dynamic coefficients of the HGJB, Reynolds equation governing a pressure field of the journal bearing is formulated. The pressure perturbation arising from the dynamic perturbations of journal displacements and velocities is then analyzed using a

Fig. 1 A herringbone groove journal bearing: grooved bearing type; and grooved journal type





variational approach (Klit et al. 1986). The detailed derivation of the pressure perturbation  $p_x, p_y, p_{\hat{x}}$  and  $p_{\hat{y}}$ , with respect to the perturbation of displacements and velocities respectively, is presented in Appendix A. The finite element model is developed to subsequently solve for the steady-state pressure field and the pressure perturbation generated in the HGJB. The pressure perturbation  $p_x, p_y, p_{\hat{x}}$  and  $p_{\hat{y}}$  is then integrated over a circumferential direction to obtain the distribution of stiffness and damping coefficients along the bearing length. The distribution of bearing coefficients, being function of the bearing position  $\hat{z}$  that measured from the bearing center along its length, are represented in a matrix form as

$$\mathbf{k} = \begin{bmatrix} k_{xx}(\hat{z}) & k_{xy}(\hat{z}) \\ k_{yx}(\hat{z}) & k_{yy}(\hat{z}) \end{bmatrix} = \int_{\theta} \begin{pmatrix} -\cos\theta \\ -\sin\theta \end{pmatrix} [p_x(\hat{z}) & p_y(\hat{z})] Rd\theta$$

and

$$\mathbf{c} = \begin{bmatrix} c_{xx}(\hat{z}) & c_{xy}(\hat{z}) \\ c_{yx}(\hat{z}) & c_{yy}(\hat{z}) \end{bmatrix} = \int_{a} \begin{pmatrix} -\cos\theta \\ -\sin\theta \end{pmatrix} [p_{\hat{x}}(\hat{z}) & p_{\hat{y}}(\hat{z})] Rd\theta,$$

(2

where  $\theta$  is the bearing angle,  $k_{xx}(\hat{z})$  and  $k_{yy}(\hat{z})$  denote the direct stiffness distributions,  $k_{xy}(\hat{z})$  and  $k_{yx}(\hat{z})$  denote the cross-coupled stiffness distributions,  $c_{xx}(\hat{z})$  and  $c_{yy}(\hat{z})$  denote the direct damping distributions, and  $c_{xy}(\hat{z})$  and  $c_{yx}(\hat{z})$  denote the cross-coupled damping distributions. The distributions of stiffness and damping coefficients in (1) and (2) have units of N/m² and Ns/m², respectively, characterizing the distributed bearing forces. Note that total stiffness and damping coefficients for the discrete bearing forces can be determined from an integration of  $k_{xx}(\hat{z}), k_{xy}(\hat{z}), c_{xx}(\hat{z})$ , and  $c_{xy}(\hat{z})$  over  $\hat{z}$ .

In general, the data of the bearing coefficients for HGJB in spindle drives are determined numerically in terms of discrete stiffness and damping coefficients, and these data are reported in various publications. Thus, the present model of distributed bearing forces was validated by comparing the *total* dynamic coefficients for the discrete bearing forces of various HGJBs with the data published in Zirkelback et al. (1998) and Jang et al. (1999), as presented in Jintanawan (2004). The difference of the bearing coefficients in the comparison is less than 8%.

A GB-type HGJB for a HDD spindle with properties and geometry shown in Table 1 is analyzed. Figure 2 shows the distribution of dynamic coefficients of this HGJB at various bearing position  $\hat{z}$ . The calculation yields  $k_{xx}(\hat{z}) = k_{yy}(\hat{z}), k_{xy}(\hat{z}) = -k_{yx}(\hat{z}), c_{xx}(\hat{z}) = c_{yy}(\hat{z})$ , and  $c_{xy}(\hat{z}) = -c_{yx}(\hat{z})$ . This so-called isotropic property occurs in the lightly loaded bearing such as the HGJB for hard disk drives. In Fig. 2, the distributions of direct and cross-coupled stiffness  $k_{xx}(\hat{z}), k_{xy}(\hat{z})$  and the distribution of direct damping  $c_{xx}(\hat{z})$  are gradually increased from both sided-ends of the bearing, and reach maximum at

Table 1 Geometry and property of the GB-type HGJB

Fluid viscosity (µ)	0.0142 Pa's
Clearance (c)	2.5 μm
Rotational speed (ω <sub>3</sub> )	7,200 rpm
Radius of journal (R)	2 mm
Groove angle (α)	157°
Groove depth ratio $(c_g/c)$	2.4
Ridge ratio $(w_r/w_r + w_g)$	0.8
Number of groove $(N_g)$	6
Bearing width to diameter ratio $(L/D)$	0.7
Eccentricity ratio $(e_0/c)$	0

the bearing center. In addition the cross-coupled stiffness  $k_{xy}(\hat{z})$  is larger than the direct stiffness  $k_{xx}(\hat{z})$ . Note that the total cross-coupled damping is about zero.

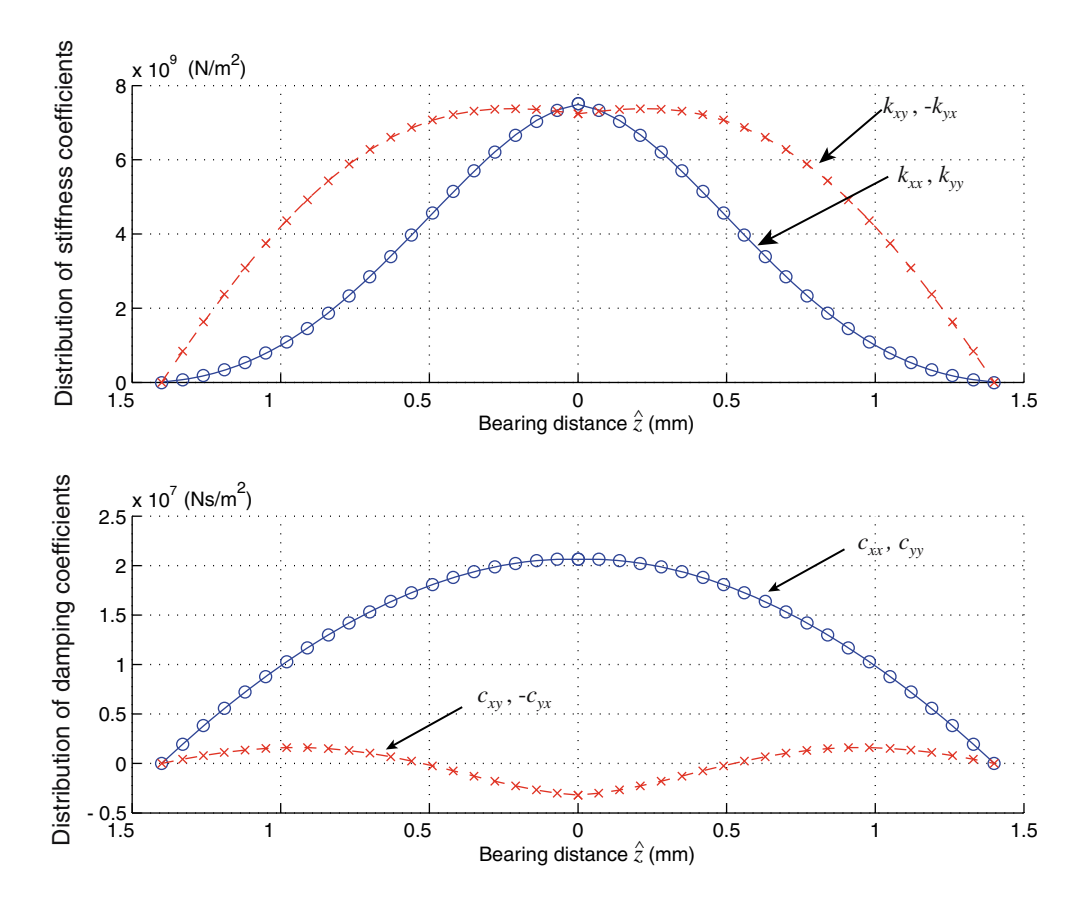
# 3 Dynamical model of FDB spindle systems with distributed bearing forces

In this section, the mathematical model of fluid dynamic bearing (FDB) spindle systems with distributed journal bearing forces, predicting the *transverse* vibration of a HDD, is presented. The equations governing the transverse motion of the spindle systems are derived using Lagrange's method. Most detailed derivation is not different from that presented in Jintanawan et al. (2001) and would be omitted here. This paper however will focus on a formulation of the distributed bearing forces provided by HGJB and a contribution of these distributed forces to the dynamical model of the system.

#### 3.1 Model description

Figure 3 shows a physical model of the FDB spindle system in HDD. The system consists of N elastic circular disks clamped to a deformable hub that allows infinitesimal rigid-body translation and rocking. The hub is press-fit onto a rotating, flexible shaft, which is mounted to the base through two HGJB and a spiralgrooved thrust bearing. The HGJBs provide distributed direct and cross-coupled spring and damping forces in the radial direction. The thrust bearing provides the axial restoring and damping forces against the spindle axial motion as well as the restoring- and dampingrocking moments against the spindle rocking. In order to provide the rocking moment to the system, the thrust bearing is modeled as torsional springs and dampers through the angular direct and cross-coupled stiffness and damping coefficients,  $k_{t1}$ ,  $k_{t2}$ ,  $c_{t1}$ ,  $c_{t2}$  (Jintanawan et al. 2001). According to large deformation of the hub around the press-fit, the hub-shaft interface is modeled as a hinged support with a torsional spring. In this model, the spindle system is axisymmetric and all the disks are identical. Only the zero-nodal-circle modes of the disk vibration are retained in the

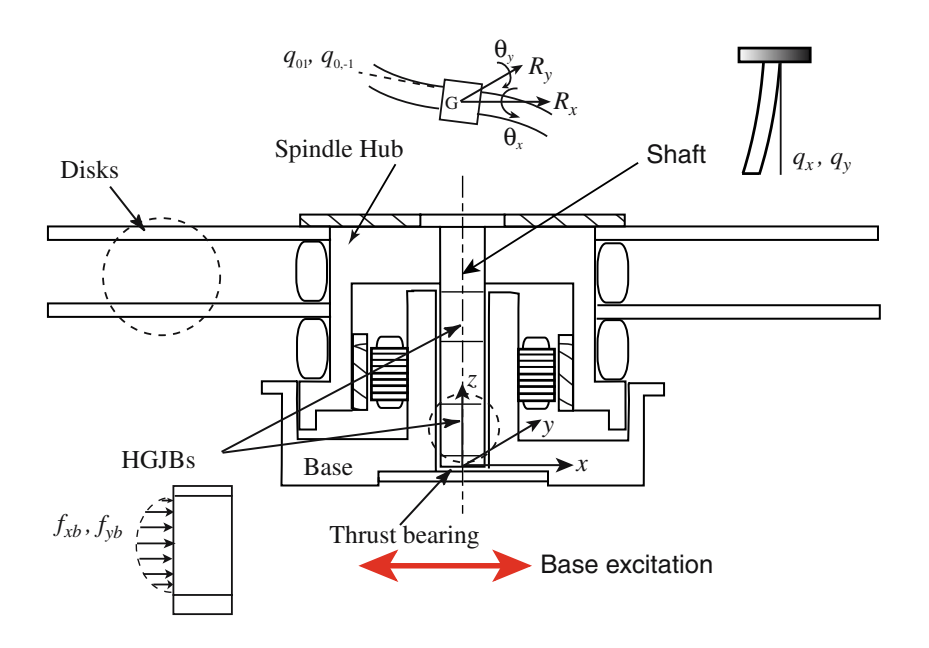
Fig. 2 Distributions of dynamic coefficients of the GB-type HGJB



mathematical model because of their significance in the frequency range of interest. Moreover, the motion of the system in the spindle's transverse and axial directions can be completely decoupled (Jintanawan 2000). In this study, the spindle spins at a constant speed  $\omega_3$  and is subjected to the base excitation in the disk-plane direction, thus the system exhibits only the transverse motion.

The transverse motion of the FDB spindle system for HDD is described by the following generalized coordinates: infinitesimal rigid body whirling of the spindle hub  $(R_x, R_y)$ ; infinitesimal rigid body precession of the hub  $(\theta_x, \theta_y)$ ; eigenmodes of the flexible shaft  $(q_x, q_y)$ ; and the (0,1) eigenmodes of each disk  $(q_{01}^{(i)}, q_{0,-1}^{(i)}, i = 1, 2, ..., N)$ .

Fig. 3 A FDB spindle system for HDD



#### 3.2 Model of distributed dynamic bearing forces in HGJB

The HGJB is modeled as generalized internal forces through distributed direct and cross-coupled stiffnesses and dampings. Let us consider a single arbitrary HGJB. An infinitesimal deflection of the bearing at various position z, (z is measured from the lower end of the shaft), can be discretized in terms of the generalized coordinates as follows:

$$\mathbf{r}_{b}(z) \equiv r_{xb}(z)\mathbf{I} + r_{yb}(z)\mathbf{J} + r_{zb}\mathbf{K}; \quad z_{lb} \leqslant z \leqslant z_{ub}$$

$$= (R_{x} + \phi(z)q_{x} + z_{b}\theta_{y})\mathbf{I} + (R_{y} + \phi(z)q_{y} - z_{b}\theta_{x})\mathbf{J}$$

$$+ R_{z}\mathbf{K}, \tag{3}$$

where **I**, **J** and **K** are the unit vectors,  $\phi(z)$  is the first modeshape or eigenfunction of the shaft,  $z_{lb}$  and  $z_{ub}$  are the positions of lower and upper ends of the bearing, and  $z_b = z - z_G$  is the bearing position that measured with respect to the system C.G. For the isotropic bearing, the distribution of stiffness and damping coefficients are simply

$$k_1(z) \equiv k_{xx}(z) = k_{yy}(z);$$
  $k_2(z) \equiv k_{xy}(z) = -k_{yx}(z);$   $c_1(z) \equiv c_{xx}(z) = c_{yy}(z);$   $c_2(z) \equiv c_{xy}(z) = -c_{yx}(z)$  (4)

$$\begin{pmatrix} f_{xb}(z) \\ f_{yb}(z) \end{pmatrix} = -\begin{bmatrix} k_1(z) & k_2(z) \\ -k_2(z) & k_1(z) \end{bmatrix} \begin{pmatrix} r_{xb}(z) \\ r_{yb}(z) \end{pmatrix} - \begin{bmatrix} c_1(z) & c_2(z) \\ -c_2(z) & c_1(z) \end{bmatrix} \begin{pmatrix} \dot{r}_{xb}(z) \\ \dot{r}_{yb}(z) \end{pmatrix}.$$
(5)

Hence the virtual work done by HGJB is

$$\delta W = \int_{z_{\text{lb}}}^{z_{\text{ub}}} f_{xb}(z) \delta r_{xb} dz + \int_{z_{\text{lb}}}^{z_{\text{ub}}} f_{yb}(z) \delta r_{yb} dz, \tag{6}$$

where  $\delta r_{xb}$  (z) and  $\delta r_{vb}$  (z) are virtual displacements of the bearing.

#### 3.3 Equations governing transverse motion

The equation governing the transverse motion of the FDB spindle system can be simplified by using the following complex representation

$$\bar{\theta} \equiv \theta_x + j\theta_y, \ \bar{R} \equiv R_x + jR_y, 
\bar{Q}_{01}^{(i)} \equiv q_{0-1}^{(i)} - jq_{01}^{(i)}, \ \bar{q} \equiv q_x + jq_y,$$
(7)

where  $j \equiv \sqrt{-1}$ . The matrix equation of motion governing the transverse motion of the system is then

$$M\ddot{\mathbf{q}}(t) + (\mathbf{G} + \mathbf{C})\dot{\mathbf{q}}(t) + \mathbf{K}\mathbf{q}(t) = \mathbf{f}(t), \tag{8}$$

where  $\mathbf{q}$  is a vector of the generalized coordinates,  $\mathbf{M}$  is the inertia matrix, G is the complex gyroscopic matrix, C is the complex damping matrix, and **K** is the complex stiffness and oscillatory matrix given by

$$\mathbf{q} = (\bar{\theta}, \ \bar{R}, \ \bar{q}, \ \bar{Q}_{01}^{(1)}, \ \bar{Q}_{01}^{(2)}, \ \dots, \ \bar{Q}_{01}^{(N)})^{\mathrm{T}}, \tag{9}$$

$$\mathbf{M} = \begin{bmatrix} \eta_1 & 0 & j\alpha_1 & a_0 & a_0 & \cdots & a_0 \\ 0 & \eta_0 & \lambda_1 & 0 & 0 & \cdots & 0 \\ -j\alpha_1 & \lambda_1 & \eta_2 & 0 & 0 & \cdots & 0 \\ a_0 & 0 & 0 & 1 & 0 & \cdots & 0 \\ a_0 & 0 & 0 & 0 & 1 & \cdots & 0 \\ \vdots & \vdots & \vdots & \vdots & \vdots & \ddots & \vdots \\ a_0 & 0 & 0 & 0 & 0 & \cdots & 1 \end{bmatrix},$$
(10)

$$\mathbf{G} = j\omega_{3} \begin{vmatrix} \eta_{3} & 0 & j\alpha_{2} & 2a_{0} & 2a_{0} & \cdots & 2a_{0} \\ 0 & 0 & 0 & 0 & 0 & \cdots & 0 \\ -j\alpha_{2} & 0 & \lambda_{2} & 0 & 0 & \cdots & 0 \\ 2a_{0} & 0 & 0 & 2 & 0 & \cdots & 0 \\ 2a_{0} & 0 & 0 & 0 & 2 & \cdots & 0 \\ \vdots & \vdots & \vdots & \vdots & \vdots & \ddots & \vdots \\ 2a_{0} & 0 & 0 & 0 & 0 & \cdots & 2 \end{vmatrix}, \tag{11}$$

$$c_{1}(z) \equiv c_{xx}(z) = c_{yy}(z); \quad c_{2}(z) \equiv c_{xy}(z) = -c_{yx}(z)$$
With  $k_{1}(z)$ ,  $k_{2}(z)$ ,  $c_{1}(z)$ , and  $c_{2}(z)$  obtained from Section 2, the distributed forces per unit length provided by
$$\mathbf{C} = \begin{bmatrix} c_{\theta\theta} & c_{\theta R} & c_{\theta q} & 0 & 0 & \cdots & 0 \\ -c_{\theta R} & c_{RR} & c_{Rq} & 0 & 0 & \cdots & 0 \\ 0 & 0 & 0 & 0 & \cdots & 0 \\ 0 & 0 & 0 & 0 & \cdots & 0 \\ 0 & 0 & 0 & 0 & \cdots & 0 \\ \vdots & \vdots & \vdots & \vdots & \vdots & \vdots \\ 0 & 0 & 0 & 0 & \cdots & 0 \end{bmatrix},$$
(12)

$$\mathbf{K} = \begin{bmatrix} k_{\theta\theta} & k_{\theta R} & k_{\theta q} & 0 & 0 & \cdots & 0 \\ -k_{\theta R} & k_{RR} & k_{Rq} & 0 & 0 & \cdots & 0 \\ -k_{\theta q} & k_{Rq} & k_{qq} & 0 & 0 & \cdots & 0 \\ 0 & 0 & 0 & k_{01} & 0 & \cdots & 0 \\ 0 & 0 & 0 & 0 & k_{01} & \cdots & 0 \\ \vdots & \vdots & \vdots & \vdots & \vdots & \ddots & \vdots \\ 0 & 0 & 0 & 0 & 0 & \cdots & k_{01} \end{bmatrix},$$
(13)

 $\mathbf{f}(t)$  is a vector of the generalized forces associated with the base acceleration  $\ddot{s}(t)$  given by

$$\mathbf{f} = \ddot{s}(t)(0, \, \eta_0, \, \lambda_1, \, 0, \, \dots, \, 0)^{\mathrm{T}}. \tag{14}$$

The distributions of coefficients  $k_1(z)$ ,  $k_2(z)$ ,  $c_1(z)$ , and  $c_2(z)$  are contributed to the components of matrices C and **K** in (12) and (13) as follows:

(7) 
$$c_{\theta\theta} = \frac{1}{I_1} \sum_{r} \left[ \int_{z_{lb}}^{z_{ub}} z_b^2(c_1 - jc_2) dz \right] + \sum_{t} C_t,$$
(8) 
$$c_{\theta R} = \frac{j}{I_1} \sum_{r} \left[ \int_{z_{lb}}^{z_{ub}} z_b(c_1 - jc_2) dz \right]$$

$$\begin{split} c_{\theta q} &= \frac{j}{I_1} \sum_r \left[ \int\limits_{z_{\mathrm{lb}}}^{z_{\mathrm{ub}}} z_b \phi(z) (c_1 - jc_2) \mathrm{d}z \right] + \sum_t \frac{\partial \phi(z_t)}{\partial z} C_t, \\ c_{RR} &= \frac{1}{I_1} \sum_r \left[ \int\limits_{z_{\mathrm{lb}}}^{z_{\mathrm{ub}}} (c_1 - jc_2) \mathrm{d}z \right], \\ c_{Rq} &= \frac{1}{I_1} \sum_r \left[ \int\limits_{z_{\mathrm{ub}}}^{z_{\mathrm{ub}}} \phi(z) (c_1 - jc_2) \mathrm{d}z \right], \end{split}$$

$$c_{qq} = \frac{1}{I_1} \sum_r \left[ \int\limits_{z_{\mathrm{lb}}}^{z_{\mathrm{ub}}} \phi^2(z) (c_1 - jc_2) \mathrm{d}z \right] + \sum_t \left[ \frac{\partial \phi(z_t)}{\partial z} \right]^2 C_t$$

where  $\sum_{\mathbf{r}} []$  and  $\sum_{\mathbf{t}} []$  are sum over all the radial HGJBs and the thrust bearings, respectively,  $C_t = c_{t1} - jc_{t2}$  is the angular damping coefficients of the thrust bearing, and  $z_t$  is the position of the thrust bearing. In addition, the coefficients  $k_{\theta\theta}$ ,  $k_{\theta R}$ ,  $k_{\theta q}$ ,  $k_{RR}$ ,  $k_{Rq}$  can be found from (15) with all c replaced by k. Also

$$k_{qq} = \omega_{s}^{2} + \frac{1}{I_{1}} \sum_{r} \left[ \int_{z_{1b}}^{z_{ub}} \phi^{2}(z)(k_{1} - jk_{2}) dz \right] + \sum_{t} \left[ \frac{\partial \phi(z_{t})}{\partial z} \right]^{2} K_{t},$$

$$(16)$$

where  $\omega_s$  is the shaft natural frequency, and  $K_t = k_t - jk_{t2}$  is the angular stiffness coefficients of the thrust bearing. Moreover, the rest detailed description of each term in **M**, **G**, **C**, **K**, and **f**(*t*) is given in Appendix B.

#### 4 Vibration analysis

In this section, free and forced vibrations of the FDB spindle systems with distributed bearing forces are analyzed for various aspect ratios of the bearing width to the shaft length. For the free vibration, natural frequencies and modal dampings of the transverse modes are present. The modal damping indicates the shape of resonance peak and characteristics of the resonance

amplitudes when subjected to the excitation. For forced vibration, transverse frequency response functions (FRF) of the system subjected to the base excitation in the disk-plane direction are present. Free and forced vibrations predicted by the model in Sect. 3 are compared to those predicted by the conventional model with discrete bearing forces (Jintanawan et al. 2001). Effect of the distributed bearing forces of HGJBs on the natural frequencies, modal dampings and transverse FRF of the spindle system is then discussed.

Two nearly identical disk-spindle systems A and B for HDD, with only difference in bearing width, are studied. Both systems have two-disk platter. Geometries and properties of the disks and spindle are listed in Table 2. Each spindle consists of two identical HGJB whose property and geometry, except L/D, are previously shown in Table 1. In addition the bearing width of spindles A and B are 2.8 and 5 mm, respectively. Thus the aspect ratios of each bearing width to the shaft length for both spindles are 0.17 and 0.30, respectively. The angular stiffness and damping coefficients of the thrust bearing are assumed small and negligible in this case.

#### 4.1 Free vibration

The model of spindle system with distributed bearing forces developed in Sect. 3 predicts the natural frequencies and the modal dampings of spindles A and B as illustrated by the solid lines in Fig. 4 for various spin speeds. In addition, these results are compared to the values predicted by the model with discrete bearing forces as shown by the dashed lines in the same plot. Furthermore, the values of the natural frequencies and the modal dampings of spindles A and B for 120 Hz spin speed that predicted by both models are presented in Tables 3 and 4. Both spindle models with either discrete or distributed bearing forces predict similar characteristics of the transverse vibration which can be divided into two groups: (a) four half-speed whirl (HSW) modes, and (b) two pairs of rocking modes; see Fig. 4. Each modeshape exhibits a coupled motion of the spindle whirling and precession, the flexible shaft vibration and

Table 2 Geometry and properties of a two-disk FDB spindle system in a hard disk drive

Disk		Spindle	_
b a I <sub>1</sub>	47.50 mm 15.24 mm 1.372 kg mm <sup>2</sup>	I <sub>1</sub> I <sub>3</sub> m	3.293 kg mm <sup>2</sup> 4.818 kg mm <sup>2</sup> 3.180×10 <sup>-2</sup> kg
z <sub>1</sub> z <sub>2</sub> m	-4.425  mm -8.245  mm $2.282 \times 10^{-2} \text{ kg}$	Shaft Length $l_s$ Diameter $d_s$ $z_{lb}$ (for lower HGJB) $z_{ub}$ (for upper HGJB) $E_s$ $\rho_s$	16.9 mm 4 mm 1.55 mm 14.87 mm 190 GPa 7,800 kg/m <sup>3</sup>

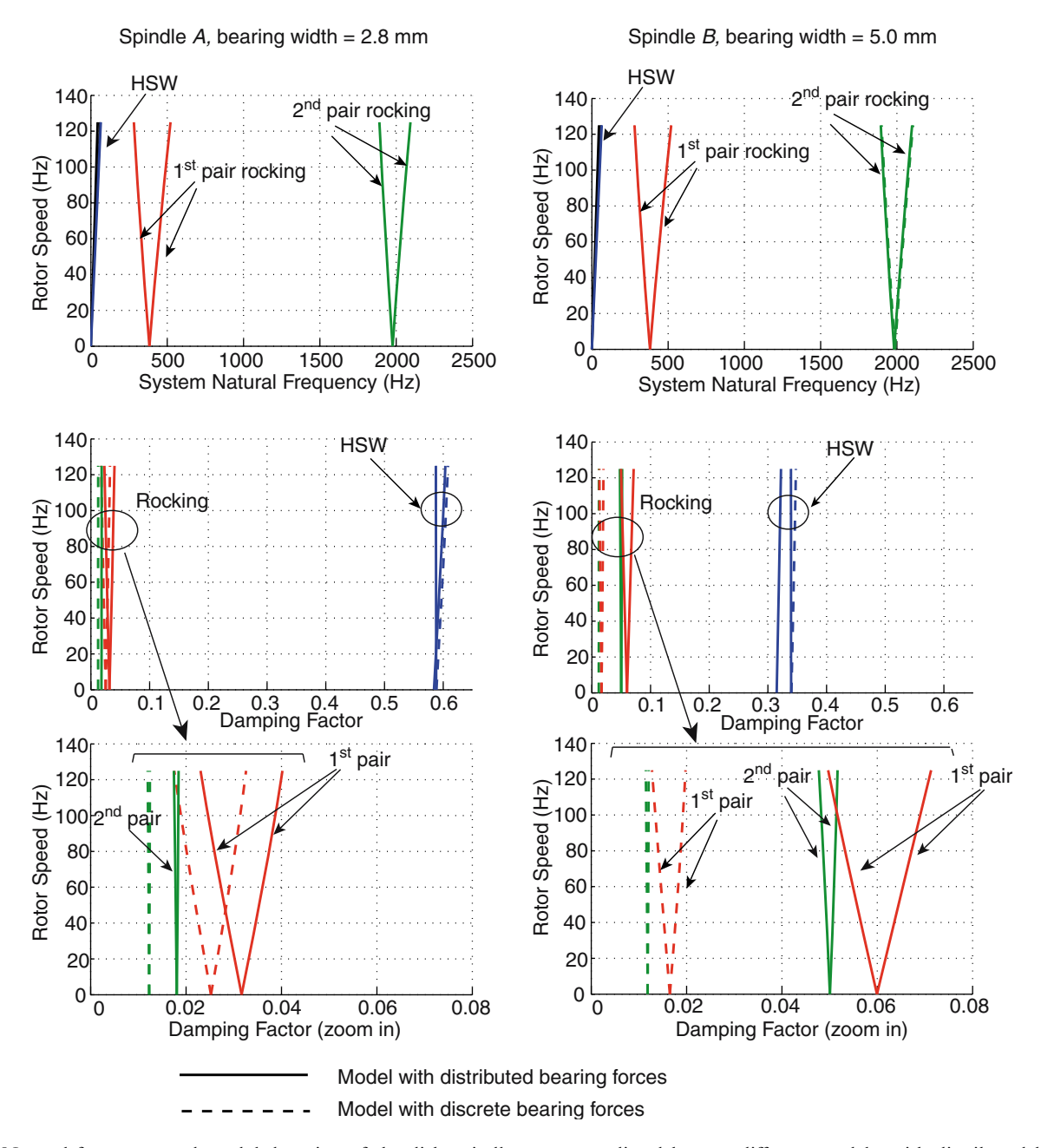


Fig. 4 Natural frequency and modal damping of the disk-spindle system predicted by two different models: with distributed bearing forces and with discrete bearing forces, for the bearing width of 2.8 and 5.0 mm

the disk vibration of (0,1) modes (Shen et al. 1997; Jintanawan et al. 1999). All these vibration modes exist in the transverse direction, and hence are the main cause of the track misregistration. In Fig. 4, the half-speed whirls occur at a certain frequency about half of the rotor speed, and they are heavily damped compared to the rocking modes. The frequencies and damping of the rocking mode pairs have two split branches known as backward (B) and forward (F) modes, as seen in Fig. 4. In addition, for both rocking mode pairs, the modal damping of the backward modes is always slightly greater than the damping of the forward modes as

shown in Tables 3 and 4. In practice, the predictable half-speed whirl can be corrected by the servo system in HDD. Therefore, it is the rocking modes that are the major concern in optimizing the vibration performance of HDD spindles. Moreover, only the spindle model considering the shaft and disk flexibility can predict these two rocking mode pairs.

Compared to the conventional model of discrete bearing forces, the spindle model with distributed bearing forces predicts the same natural frequencies for all transverse modes but predicts higher modal dampings of the rocking mode pairs. The difference in damping

**Table 3** Natural frequencies and modal dampings of spindle A (bearing width = 2.8 mm)

Vibration modes	Natural frequencies (Hz)		Modal damping (%)	
	Discrete model	Distributed model	Discrete model	Distributed model
HSW	62.5	62.5	60	60
Rocking B1	285	285	3.23	3.99
Rocking F1	515	515	1.78	2.33
Rocking B2	1893	1893	1.24	1.84
Rocking F2	2089	2088	1.20	1.75

**Table 4** Natural frequencies and modal dampings of spindle B (bearing width = 5.0 mm)

Vibration modes	Natural frequencies (Hz)		Modal damping (%)	
	Discrete model	Distributed model	Discrete model	Distributed model
HSW	62	62	34	32
Rocking B1	282	283	1.97	7.09
Rocking F1	513	514	1.29	5.01
Rocking B2	1902	1897	1.20	5.16
Rocking F2	2100	2094	1.15	4.78

prediction is clearer for spindle *B* where the ratio of the bearing width to the shaft length becomes larger. It implies that under the base excitation, the resonance peaks of the rocking modes predicted by the model with distributed bearing forces are more heavily damped (the peaks are less steep) and the rocking amplitude is smaller when compared to those predicted by the conventional model of discrete bearing force. In the spindle design, the rocking amplitudes have to be minimized in order to optimize the vibration performance. With the higher modal damping of the rocking modes, the vibration performance of HDD spindles is better.

The same predictions of natural frequency for both models can be explained as follows. The half-speed whirls are an inherence whirl phenomena of the bearing and their resonance frequency is only affected by the spin speed. Furthermore, the frequencies of the rocking mode pairs substantially depend on the natural frequencies of the shaft and disk ( $\omega_s$  and  $\omega_{01}$ ) through the terms  $k_{qq}$  and  $k_{01}$  in (13) and (16). Accordingly, the bearing property and geometry has no great effect on all resonance frequencies. The difference in damping predictions of the rocking modes from the two models can be discussed as follows. The modal damping of the rocking modes is mainly affected by the damping in the bearing as well as the bearing deflection, through the terms  $c_{\theta\theta}$ ,  $c_{\theta R}$ ,  $c_{\theta q}$ ,  $c_{RR}$ ,  $c_{Rq}$ , and  $c_{qq}$  in (15). For the distributed bearing forces, the bearing deflection is considered as continuously varied along the bearing length due to the shaft flexibility. Thus, it results in different values of modal dampings compared to those predicted by the spindle model with discrete bearing forces that the bearing deflection is simply evaluated at the bearing center.

To further investigate the effect of shaft flexibility on the modal damping that predicted by the model with distributed bearing forces, Fig. 5 compares the natural

frequencies and modal dampings<sup>1</sup> of two different flexible-disk spindle systems: (1) with rigid shaft; and (2) with flexible shaft, for various spin speed. When compared to the flexible-shaft system, the system with rigid shaft possesses four half-speed whirl modes but only one pair of rocking modes. This is because of reduced degrees of freedom in the system. Moreover, the modal dampings of rocking modes for the rigid-shaft spindle system, predicted by the models with either discrete or distributed bearing forces, are nearly identical, as seen on the left of Fig. 5. It is implied that the model of distributed bearing forces does not cause any difference in damping prediction unless the shaft is flexible. For the rigid shaft, the deflection of the bearing, which is affected by only the whirling and the rocking of the rigid spindle, slightly varies along its length. In such case, the dynamic resultants of bearing forces obtained from either discrete or distributed models are not different, and hence resulting in similar vibration characteristics.

For the FDB spindle system with significant aspect ratio of the bearing width to the shaft length and the shaft is likely flexible, the conventional spindle model with discrete bearing forces would not accurately predict the modal damping of rocking modes. In such system, the dynamic model of disk—spindle system with distributed bearing forces could be the alternative model for improving the damping prediction.

#### 4.2 Forced vibration

In this section, we present a simulation of frequency response functions (FRF) whose response is measured from the disk along the radial or transverse direction,

<sup>&</sup>lt;sup>1</sup>For all cases, the modal dampings of the half-speed whirl modes are not different, and hence they are not shown in Fig. 5

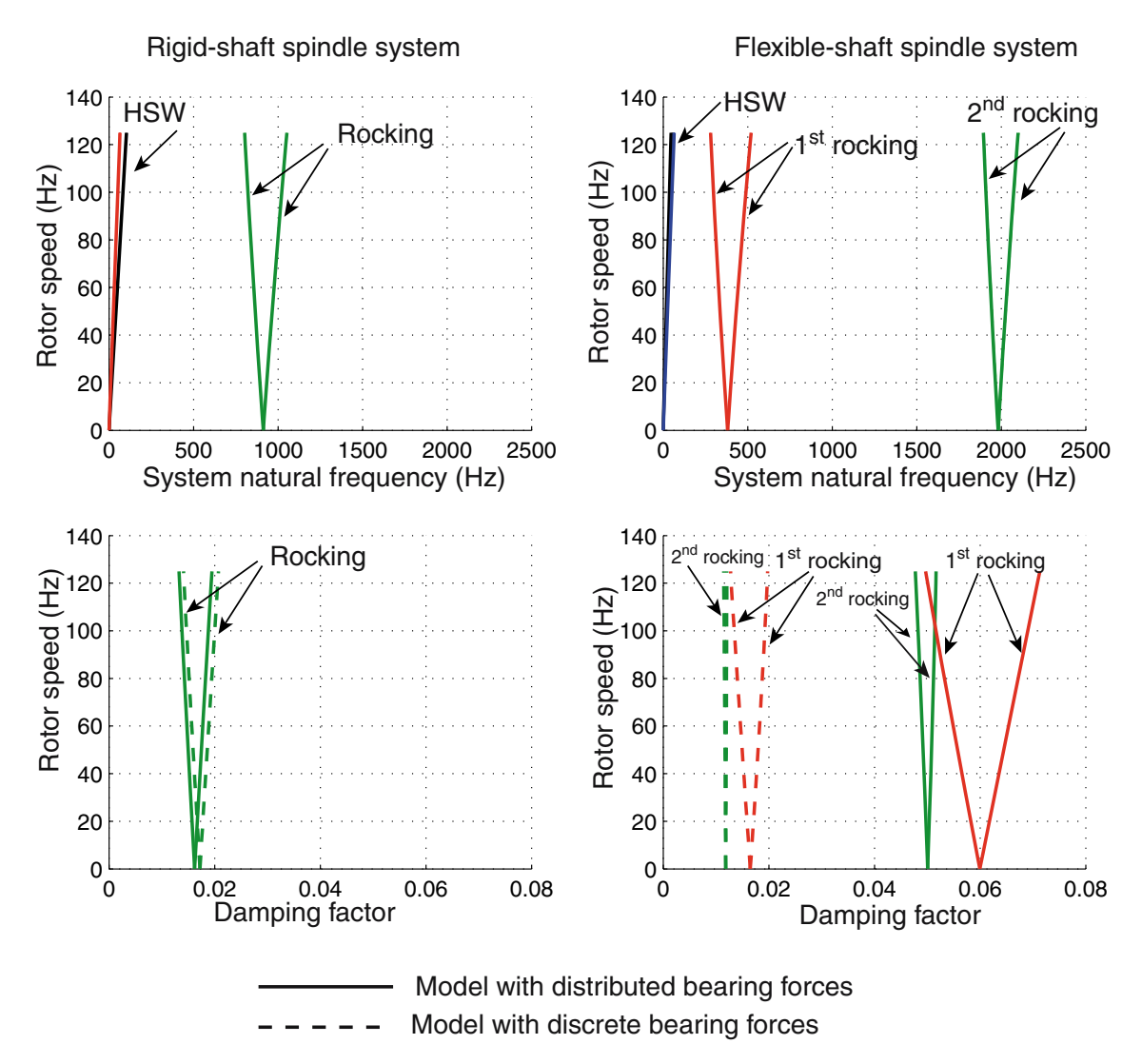


Fig. 5 Free vibration prediction of the rigid-shaft and flexible-shaft spindle systems with the bearing width of 5.0 mm

when subjected to the base excitation in the disk-plane direction. This transverse FRF well represents the possible track-misregistration in HDD and can be expressed as:

$$\vec{\Delta}(z) \equiv \Delta_x(z)\mathbf{I} + \Delta_y(z)\mathbf{J} 
= (R_x + z_0\theta_y)\mathbf{I} + (R_y - z_0\theta_x)\mathbf{J}'$$
(17)

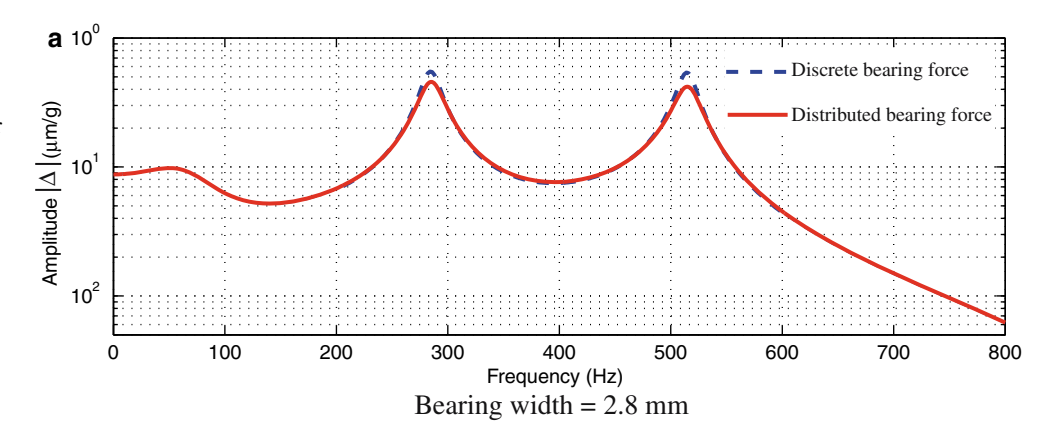
where  $z_0 = z - z_G$  is the distance of the measurement level from system C.G. This transverse vibration consists of two components: one from the spindle whirling  $(R_x \text{ and } R_y)$  and the other from the spindle precession  $(z_0\theta_y)$  and  $z_0\theta_x$ ).

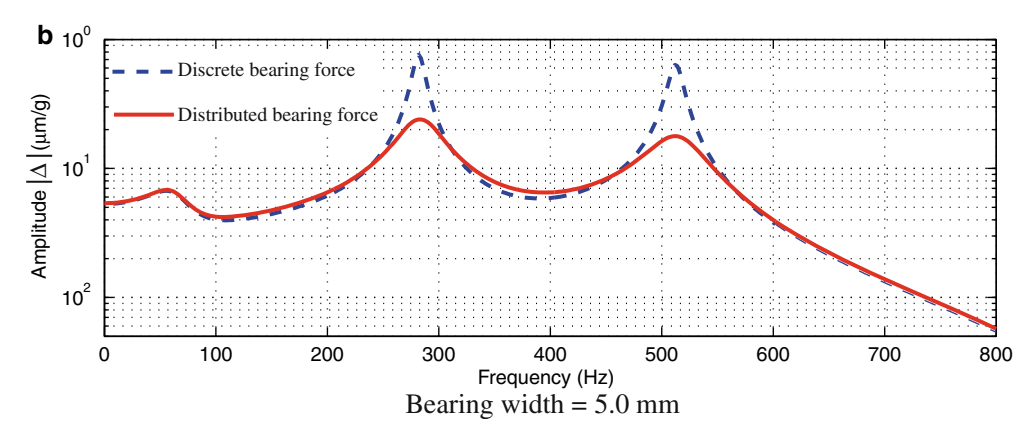
Figure 6 shows the magnitudes of transverse FRF  $|\overline{\Delta}|$  of the previously described disk-spindle systems A and B, when the response is measured from the lower disk and the spindle spins at 7,200 rpm or 120 Hz. In Fig. 6 the transverse FRF of both systems A and B that predicted by the spindle models with discrete and distributed bearing forces are compared. In all cases, for the

frequency range of 0–800 Hz there exist the resonance peaks of half-speed whirl modes at 60 Hz and the first pair of backward and forward rocking modes at 270 and 520 Hz. Moreover, the resonance peaks of rocking modes predicted by the present model with distributed bearing forces are more heavily damped. The larger damping of rocking modes is much clearer for the case of system *B* with wider bearing width.

Note that the resonance peak of the half-speed whirls at 60 Hz as presented in Fig. 6 is more heavily damped when qualitatively compared to the peaks from general test results (e.g., Fig. 8 in Jintanawan et al. 2001). The observation reveals that the predicted modal damping of the half-speed whirl might be too high. In the parametric study (Park et al. 2002), the half-speed whirl damping is decreased with the lower direct stiffness of HGJB. Similarly, the damping of the half-speed whirl might decrease due to the flexibility of the stationary base (Tseng et al. 2003), which is not included in this model. The base flexibility would yield less stiffness of the structure

Fig. 6 Transverse FRF of the disk—spindle system predicted by two different models: with distributed bearing forces and with discrete bearing forces, for the bearing width of 2.8 and 5.0 mm





that leads to the smaller damping of the half-speed whirl mode for the actual system. In addition, to accurately predict the half-speed whirls, the exact values of bearing properties such as viscosity, clearance, and length, etc., are needed for calculating the bearing coefficients. Acknowledgments The valuable discussion from Prof. I. Y. (Steve) Shen, Department of Mechanical Engineering, University of Washington, is gratefully acknowledged. This research is supported by the "Research Grant for New Scholars-MRG4880174" from Thailand Research Fund (TRF).

#### **5 Conclusions**

In this paper we present a dynamical model of diskspindle systems with distributed forces in HGJB for predicting transverse vibration of HDD spindles. When compared to vibration predicted by the conventional spindle model with discrete bearing forces, the present model with distributed bearing forces predicts the same natural frequencies for all transverse modes but higher modal damping of the rocking modes. The difference in damping prediction is clearer when the aspect ratio of the bearing width to the shaft length becomes larger and the shaft is likely flexible. Specifically, the modal damping of the rocking modes is substantially affected by the journal bearing forces. For the present model, these bearing forces are distributed along the bearing length where the bearing deflection is continuously varied due to the shaft flexibility. The spindle model with distributed bearing forces could be the alternative model for improving the damping prediction of the rocking modes.

#### Appendix A

Consider an arbitrary herringbone grooved journal bearing (HGJB) as shown in Fig. 1. The inertial coordinate system xy describes the motion of the journal center and the coordinate system  $\hat{x}\hat{z}$  where  $\hat{x}=R\theta$  describes the position of the unwrapped fluid film. With the grooves moving, the  $\hat{x}$ -axis for the GJ-type bearing is fixed to the rotating journal. In addition it is easier to consider the journal of the GJ-type bearing as relatively stationary while the bearing sleeve rotates in the opposite direction (Zirkelback et al. 1998). The Reynolds equation governing the pressure field p in HGJB is

$$\frac{1}{R^2} \frac{\partial}{\partial \theta} \left( \frac{h^3}{12\mu} \frac{\partial p}{\partial \theta} \right) + \frac{\partial}{\partial \hat{z}} \left( \frac{h^3}{12\mu} \frac{\partial p}{\partial \hat{z}} \right) 
= L(p) = \frac{\omega_3}{2} \frac{dh}{d\theta} + \frac{\partial h}{\partial t}, \quad \text{for GB type} 
= -\frac{\omega_3}{2} \frac{dh}{d\theta} + \frac{\partial h}{\partial t}, \quad \text{for GJ type}$$
(18)

where  $\mu$  is the fluid viscosity, and h is the film thickness in the ridge and groove regions expressed respectively as

$$h = c + e_x \cos \Theta + e_y \sin \Theta \tag{19}$$

and

$$h = c + c_g + e_x \cos \Theta + e_y \sin \Theta. \tag{20}$$

In (19) and (20), c is the nominal film clearance,  $c_g$  is groove depth,  $e_x$  and  $e_y$  are journal eccentricities, also  $\Theta = \theta$  for the GB-type HGJB, and  $\Theta = \theta + \omega_3 t$  for the GJ-type HGJB. The pressure field p satisfies the following boundary conditions:  $p(\theta, \hat{z}, t) = p(\theta + 2\pi, \hat{z}, t)$  and  $p(\theta, L/2, \hat{z}) = p(\theta, -L/2, \hat{z}) = p_a$ , where  $p_a$  is the atmospheric pressure.

For a small perturbation  $\Delta e_{\sigma}$  (t), ( $\sigma = x, y$ ), of journal displacements from the steady state configuration ( $e_{x0}, e_{y0}$ ), the film thickness is then

$$h = h_0 + \Delta e_x \cos \Theta + \Delta e_y \sin \Theta = h_0 + \sum_{\sigma} \Delta e_{\sigma} h_{\sigma};$$
  
 $\sigma = x, y,$ 

where  $h_0$  is the film thickness for the steady state configuration  $(e_{x0}, e_{y0})$ ,  $h_x = \cos \Theta$ , and  $h_y = \sin \Theta$ . With the small perturbed displacement  $\Delta e_{\sigma}(t)$  and perturbed velocity  $\Delta \dot{e}_{\sigma}(t)$ ,  $(\sigma = x, y)$ , the perturbed pressure field is then

$$p = p_0 + \sum_{\sigma} p_{\sigma} \Delta e_{\sigma} + \sum_{\dot{\sigma}} p_{\dot{\sigma}} \Delta \dot{e}_{\sigma}; \quad \sigma = x, y,$$
 (23)

where  $p_{\sigma}$  and  $p_{\dot{\sigma}}(\sigma=x,y)$  are pressure perturbation with respect to the perturbed displacement and velocity, respectively. Substituting (22) and (23) into (18) and neglecting the higher order terms, the differential equation governing the steady-state pressure field is obtained as

$$L(p_0) = \frac{\omega_2}{2} \frac{dh_0}{d\theta}, \quad \text{for GB type,}$$
  
=  $-\frac{\omega_2}{2} \frac{dh_0}{d\theta} - \Omega [e_{x0} \sin \Theta - e_{y0} \cos \Theta], \cdot$   
for GJ type (24)

Moreover for both GB- and GJ-types, the equations governing the pressure perturbation are then

$$\begin{split} L(p_{\sigma}) &= \frac{\omega_{3}}{2} \frac{dh_{\sigma}}{d\theta} - \frac{1}{R^{2}} \frac{\partial}{\partial \theta} \left( \frac{3h_{0}^{2}h_{\sigma}}{12\mu} \frac{\partial p_{0}}{\partial \theta} \right) - \frac{\partial}{\partial \hat{z}} \left( \frac{3h_{0}^{2}h_{\sigma}}{12\mu} \frac{\partial p_{0}}{\partial \hat{z}} \right); \\ \sigma &= x, y, \end{split}$$

(2.5

$$L(p_{\dot{\sigma}}) = h_{\sigma}; \quad \sigma = x, y.$$

#### Appendix B

In (10) to (14),  $\eta_0$ ,  $\eta_1$ ,  $\eta_2$ ,  $\eta_3$ ,  $\lambda_1$ ,  $\lambda_2$ ,  $\alpha_1$ ,  $\alpha_2$ , and  $\alpha_0$  are the inertias normalized with respect to the diametral mass moment of inertia of each disk  $I_1$ , given by

$$\eta_{0} = \frac{M}{I_{1}}, \quad \eta_{1} = \frac{\bar{I}_{1}}{I_{1}}, \quad \eta_{2} = \frac{\hat{I}_{s}}{I_{1}}, \quad \eta_{3} = \frac{\bar{I}_{3}}{I_{1}}, 
\lambda_{1} = \frac{M_{s1}}{I_{1}}, \quad \lambda_{2} = \frac{M_{s2}}{I_{1}}, \quad \alpha_{1} = \frac{N_{s1}}{I_{1}}, \quad \alpha_{2} = \frac{N_{s2}}{I_{1}}, 
a_{0} = \frac{\pi\rho h}{I_{1}} \int_{a}^{b} R_{01}(r) r^{2} dr$$
(26)

where M is the total mass of the spindle system,  $\bar{I}$  and  $\bar{I}_3$  are the centroidal mass moment of inertia of the rotating part about x and y axes, and  $M_{s1}$ ,  $M_{s2}$ ,  $N_{s1}$ ,  $N_{s2}$ , and  $\hat{I}_s$  are the modal mass of the shaft defined in Jintanawan (2000)

In (13)  $k_{01} = \omega_{01}^2 - \omega_3^2 - j\zeta\omega_3$ , where  $\omega_{01}$  and  $\zeta$  is the natural frequencies and the normalized viscous damping of the disks as defined in Jintanawan (2000).

#### References

Booser ER (1984) Handbook of lubrication, volume I and II, CRC Press, Florida

Jang G, Kim Y (1999) Calculation of dynamic coefficients in hydrodynamic bearing considering five degree of freedom for a general rotor-bearing system. ASME J Tribol 121: 499–505

Jintanawan T (2000) Vibration of rotating disk/spindle systems with hydrodynamic bearings. PhD dissertation, University of Washington

Jintanawan T (2004) A model of distributed dynamic forces in herringbone grooved journal bearing. Proceedings of 1st International Conference on Advanced Tribology

Jintanawan T, Shen IY, Ku C-P (1999) Free and forced vibrations of a rotating disk pack and spindle motor system with hydrodynamic bearings. J Information Storage and Processing Systems 1:45–58

Jintanawan T, Shen IY, Tanaka K (2001) Vibration analysis of fluid dynamic bearing spindles with rotating-shaft design. IEEE Trans on Magn 37:799–804

Klit P, Lund JW (1986) Calculation of the dynamic coefficients of a journal bearing using a variational approach. ASME J Tribol 108: 421–425

Park JS, Shen IY, Ku C-P (2002) A parametric study on rocking vibration of rotating disk/spindle systems with hydrodynamic bearings. Microsyst Technol 8: 427–434

Shen IY; Ku C-P (1997) A nonclassical vibration analysis of multiple rotating disk/spindle system. ASME J Appl Mech 64: 165–174

Tseng CW; Shen JY; Shen IY (2003) Vibration of rotating-shaft HDD spindle motors with flexible stationary parts. IEEE Trans on Magn 39:794–799

Zirkelback N; San Andres L (1998) Finite Element analysis of herringbone grooved journal bearings: a parametric study. ASME J Tribol 120:234–240

# EFFECTS OF DISTRIBUTED BEARING FORCES AND BEARING LOCATIONS ON ROCKING VIBRATION OF FDB SPINDLE SYSTEMS

Thitima Jintanawan<sup>1</sup>

Department of Mechanical Engineering, Chulalongkorn Univeristy Phayathai Rd., Bangkok, 10330, Thailand Thitima.J@chula.ac.th

#### Introduction

Fluid dynamic bearings (FDB) are currently used in hard disk drive (HDD) spindles because of their capability in vibration and acoustic reduction. The spindle vibration in transverse direction, as known as rocking vibration, is the main cause of the track misregistration that limits the performance of storage density in HDD. The property and locations of the radial FDBs, which are the herringbonegrooved journal bearing (HGJB) type, play an important role in optimizing such unwanted rocking vibration [1]. To accurately predict the rocking vibration and optimize the bearing locations in HDD spindles, the unique geometry of the bearing-spindle in HDD needs to be considered. For disk drives with small form factors, e.g., 0.85-inch drive to be used in cell phones, most of the shaft length is supported by the bearings. In this case the aspect ratio of the bearing width to the shaft length is significant. Moreover the shaft in the rotating-shaft design spindles is likely flexible. With these observations, the HGJBs in HDD spindles would rather function as a continuous support providing distributed restoring and damping forces.

This paper is to investigate the effects of distributed bearing forces and locations of HGJBs on the rocking vibration of the FDB spindle systems. In addition the discrepancy in predicting the rocking vibration with the model of distributed bearing forces is investigated by comparing the natural frequencies, modal damping, and frequency response functions predicted by this model to the values from the conventional model of discrete bearing forces.

#### **Dynamic Model**

Figure 1 shows the physical model of the disk-spindle system with distributed bearing forces in HDD. The mathematical model is developed to predict the rocking vibration of this spindle system. The model is mainly based on the existing dynamic model [2], consisting of the rotating and flexible shaft that pressed fit to the rigid spindle hub, and the rotating flexible disks clamped on the outer rim of the hub. The HGJBs are however modeled as *distributed* direct and cross-coupled, linear spring and damping forces through the distribution functions of dynamic coefficients.

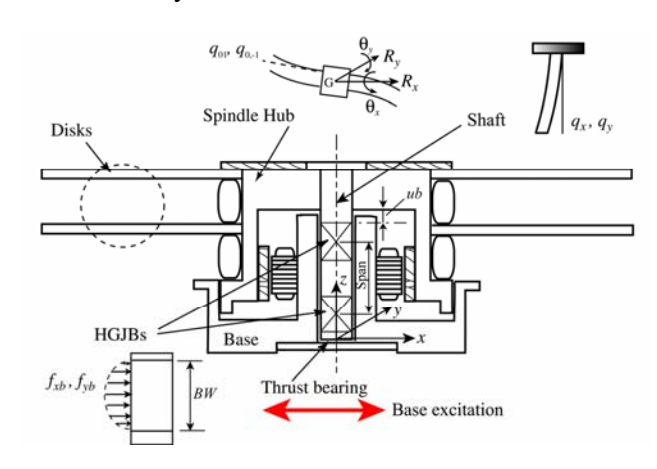


Fig.1 Physical model of disk-spindle system

#### **Free Vibration Analysis**

A standard 3.5-inch drive with two identical HGJBs and two disks is the case for study. The rocking modes predicted by the distributed bearing model can be divided into two groups: 1) half-speed whirl (HSW) modes, and 2) two pairs of (0,1) unbalanced backward and forward modes (denoted by B1, F1, B2 and F2). Natural frequencies and modal damping of the rocking modes that predicted by both models of distributed and discrete bearing forces are compared in Table 1 for two spindles with bearing widths (BW) of 2.8 and 5.0 mm, and at zero and 7200 rpm speed. Compared to the conventional model, the spindle model with distributed bearing forces

Corresponding author: Thitima Jintanawan, thitima.j@chula.ac.th

predicts the same natural frequencies for all rocking modes but predicts higher modal damping of B1, F1, B2 and F2. The difference in damping prediction of these modes is clearer for the case of larger bearing width (BW = 5.0 mm).

@ stationary (zero speed)

(Lette speed)							
Mode	BW = 2.8  mm		BW = 5.0  mm				
	$\omega_n$ (Hz)	ζ(%)	$\omega_n$ (Hz)	ζ(%)			
B1&F1	383/383	3.16/2.52	381/380	5.99/1.65			
B2&F2	1977/1977	1.81/1.23	1982/1987	5.01/1.18			

@ 7200 rpm

Mode	BW = 2.8  mm		BW = 5.0  mm	
	$\omega_n$ (Hz)	ζ(%)	$\omega_n$ (Hz)	ζ(%)
HSW	63/63	60/60	62/62	32/34
B1	285/285	3.99/3.23	283/282	7.09/1.97
F1	515/515	2.33/1.78	514/513	5.01/1.29
B2	1893/1893	1.84/1.24	1897/1902	5.16/1.20
F2	2094/2089	1.75/1.20	2094/2100	4.78/1.15

(Note: #1/#2 in the table is the value predicted by distributed model per the value predicted by conventional discrete model)

Table 1 Predicted natural frequencies and damping

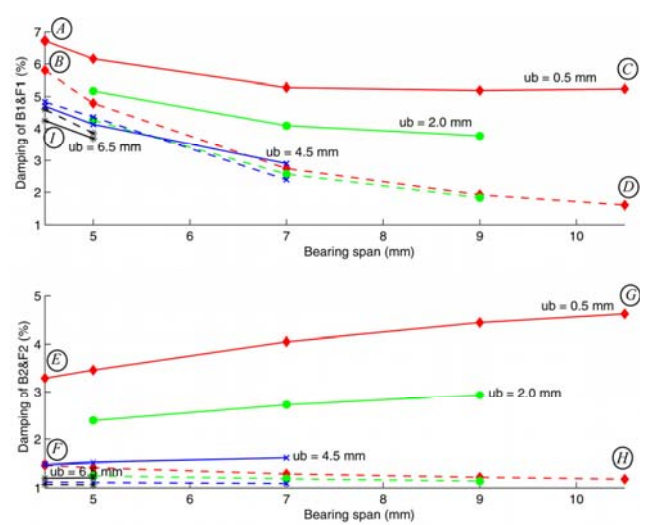
#### **Bearing Locations vs. Damping**

Fig. 2 presents the damping values of B1-F1 and B2-F2 of the stationary drive with 4.0 mm bearing width at various HGJB locations. The locations of the two HGJBs as shown in Fig. 1 are indicated by two parameters: 1) bearing span and 2) position of the upper bearing (ub) that measured from the top end of shaft. Comparing the dampings obtained from both distributed and discrete models, the discrepancy in damping prediction is greater when the span is wider and level of the upper bearing is higher (C vs. D and G vs. H in Fig. 2). The damping predicted by the distributed model depends on the locations of the bearings as described as follows. With a certain level of the upper bearing but wider span, the damping of B1&F1 is decreased (A to C) whereas the damping of B2&F2 is increased (E to G). Moreover with a fixed span but the upper bearing located at higher level, the dampings of both B1&F1 and B2&F2 are increased (A vs. I and E vs. F).

#### **FRF of Rocking Vibration**

The modal dampings presented in Fig. 2 indicate the shape and the amplitude of the rocking resonance in the frequency response function (FRF) as shown, for examples, in Fig. 3. The peaks around 400 Hz and 2 KHz in Fig. 3 are the *B*1-*F*1 and *B*2-*F*2, respectively. With the larger span or the decrease in level of the upper bearing, the system is more flexible as the natural frequencies are decreased. When the bearing span is wider (I vs. II in Fig.

3), the amplitude of B1-F1 is increased while the amplitude of B2-F2 is decreased. This respectively corresponds to the decrease and increase of damping by  $\sim 1\%$ . In addition an increase in level of the upper bearing results in a more heavily damped peaks, and hence a decrease of the resonance amplitudes (II vs. III).



**Fig.2** Effects of HGJB locations to the damping of B1&F1, B2&F2 @ stationary (solid lines represent distributed model; dashed lines represent discrete model)

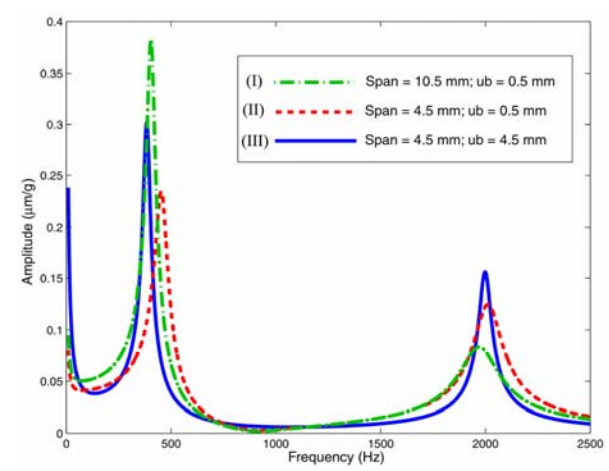


**Fig.3** Transverse FRF of the stationary drive with distributed bearing forces subjected to base excitation

#### References

- [1] Park, J. S., Shen, I. Y. and Ku, C.-P. R.., 2002, "A parametric study on rocking vibration of rotating disk/spindle systems with hydrodynamic bearings: rotating-shaft design," *Microsystem Technologies*, 8:427-434.
- [2] Jintanawan, T., Shen, I. Y. and Tanaka, K., 2001, "Vibration analysis of fluid bearing spindles with rotating-shaft design," *IEEE Trans. Magn.*, 37:799-805.